2013

Distribution, Variability, and Trends in Wind Characteristics in New England Coastal Areas

Kelly I. Knorr
University of Rhode Island, kellyireneknorr@gmail.com

DISTRIBUTION, VARIABILITY, AND TRENDS IN WIND CHARACTERISTICS IN NEW ENGLAND COASTAL AREAS

BY

KELLY I. KNORR

A THESIS SUBMITTED IN PARTIAL FULFILLMENT OF THE REQUIREMENTS FOR THE DEGREE OF

MASTER OF SCIENCE

IN

OCEANOGRAPHY

UNIVERSITY OF RHODE ISLAND

2013

MASTER OF SCIENCE THESIS

OF

KELLY I. KNORR

APPROVED:

Thesis Committee:

Major Professor John Merrill

Annette Grilli

Brice Loose

Nasser Zawia
DEAN OF THE GRADUATE SCHOOL

UNIVERSITY OF RHODE ISLAND

2013

ABSTRACT

A comprehensive analysis of regional near-surface wind speed characteristics is presented based on data from 9 coastal sites, extending over periods of 20 to 39 years, with a mean duration of 33 years. Six terrestrial data sets were obtained from the National Climatic Data Center (NCDC), and 3 additional buoy data sets came from the National Data Buoy Center (NDBC). Data sets contain either sub-hourly or hourly wind speed averages from near-surface, single height anemometers. Extensive quality checks were performed to account for anemometer height changes, missing data, and flagged data.

Analyses focus on long-term temporal trends. Monthly, seasonal, and interannual long-term trends are analyzed utilizing low-order Gaussian moments and the Ordinary Linear Regression (OLR) technique; data autocorrelation is accounted for and additional statistical analysis is performed herein. Four sites exhibit statistically significant negative wind speed trends, 2 sites show statistically significant increased trends, and no trend is observed at 3 sites. Further data analyses include calculation of the 5th, 10th, 25th, 50th, 75th, 90th, and 95th percentiles of annual wind speeds and long-term temporal trends in the Weibull Probability Density Function (PDF) and the shape and scale parameters that describe the form of the distribution. The spatial variation of near-surface wind speed characteristics and regional wind speed climatology are also investigated.

Results indicate marked stilling in the annual mean, Weibull scale parameter, and 5th and 95th percentile values of wind speed at most terrestrial sites; opposite trends are generally observed at buoys and marine sites. Possible attributions of the source of the wind speed trends are also discussed.

ACKNOWLEDGMENTS

Thank you Jesus, my Lord and Savior. You carried me through the last 6 months!

My advisor John Merrill provided countless hours of assistance with his knowledge and personal mentorship. My other committee members Annette Grilli and Brice Loose deserve acknowledgement, too, for their time spent helping me with this study. I'd like the acknowledge my funding sources, the U.S. Navy and the Department of Energy.

Thank you to those who provided informal advice. My parents, especially my mother, and my boyfriend Eric never ceased encouraging me. I was also blessed with a wonderful SURFO Kayla Flynn. Clara and Christian, thank you for helping me with my AGU poster presentation and data analysis!

Do you not know that in a race all the runners run, but only one gets the prize? Run in such a way as to get the prize. Everyone who competes in the games goes into strict training. They do it to get a crown that will not last, but we do it to get a crown that will last forever.

1 Corinthians 9:24-25

TABLE OF CONTENTS

Page

LIST OF TABLES

LIST OF FIGURES

Figure **Page**

CHAPTER 1

Introduction

1.1 Near-surface wind

My interest is in surface winds as a fundamental variable in physical processes in the ocean and atmosphere, but I recognize that near-surface winds influence many disciplines. Climate variables in terrestrial and oceanic environments, wind energy generation, and construction and other industries are all directly affected by surface wind speeds.

Winds and the environment

Surface wind speeds, among other meteorological variables, influence the hydrological cycle through pan evaporation and crop reference evapotranspiration (Rayner, 2007; McVicar et al., 2012). Thus, understanding of the role of wind in surface flux is important for surface energy balance estimations (Monahan, 2006; Rayner, 2007). The atmospheric transport of aerosols, specifically iron which can be a limiting micronutrient, is controlled by winds (Mahowald et al., 2000). Aerosols associated with pollution and pollination are advected and deposited by winds (Okubo and Levin, 1989; Bernard et al., 2001). Heat and moisture are transported by winds; converging and diverging winds initiate convection (Capps and Zender, 2008). Near-surface ocean currents are forced by winds, and winds play a large role in air-sea interaction (Wanninkhof et al., 2002) and gas fluxes (Donelan et al., 2002). Wind speed estimates are used in storm surge and wave height forecasting for coastal protection and erosion mitigation (Bijl, 1997; Caires and Sterl, 2005). Winds are important in atmospheric modeling and large scale model projections of climate change. A modest change in initial and boundary conditions in General Circulation Models (GCMs) can significantly alter run

and ensemble responses (Capps and Zender, 2008; McVicar et al., 2012).

Wind energy production and other industries

Even though turbine hubs are typically at or above 80m and most surface anemometers measure winds speeds at 10m, wind speeds at the two heights can be related by wind power laws (Peterson and Hennessey, 1978). Therefore, wind power production is directly affected by near surface wind speeds. In addition, wind power density varies with the cube of wind speed: a seemingly minor shift in wind speeds can manifest as a substantial change in wind power (Greene et al., 2012b). As more communities lean on alternative energy and countries encourage and enforce renewable energy development, accurate wind energy assessment is needed. Wind risk assessment is a factor in the construction, marketing, and insurance of properties. For instance, winds are considered during infrastructure planning and in structural engineering techniques (Cook, 1986; Jungo et al., 2002). In addition, winds shape the location, design, and capacity of airports (Wever, 2012). Planting, harvest, and crop yield in the agricultural industry are influenced by meteorological processes directly related to near surface wind speeds (O'Neal et al., 2005).

Recent studies

Several studies in the climate literature have examined surface wind speeds. For instance, Klink (2002) analyzed interannual variability and long-term trends, Wan et al. (2009) reported spatial patterns after data homogenization, and Yan et al. (2002) and Smits et al. (2005) studied extreme surface wind speeds linked to cyclones. Recently, Pryor et al. (2009) compared in situ wind speed observations to reanalysis data sets and model outputs. These studies and others suggest that a changing climate will likely alter surface wind speeds (Vautard et al., 2010).

1.2 Are wind speeds decreasing?

It has been hypothesized that wind speeds have decreased in the past 30-50 years (McVicar et al., 2012). This phenomenon of reduced wind speeds, termed "stilling" by Roderick et al. (2007), has been identified at multiple sites in the both hemispheres over the past several decades. Reduced wind speed trends were identified in Northern Hemisphere countries including China (Xu et al., 2006), the Czech Republic (Brazdil et al., 2009), and the Netherlands (Smits et al., 2005; Wever, 2012). Studies in the Southern Hemisphere including 2 sites in Brazil (da Silva et al., 2010) and 14 in Argentina and Chile (Mahowald et al., 2007; Vautard et al., 2010) document negative trends. Furthermore, 41 sites in Australia exhibited a mean trend of -0.010 $ms^{-1}a^{-1}$ over the study period 1975-2004 (Roderick et al., 2007).

Several studies have documented reduced wind speeds in the continental United States and one study observed similar trends regionally in New England. Klink (1999; 2002) conducted wind speed metric studies in and near Minnesota and Greene et al. (2012a; 2012b) documented pronounced negative trends in winter and spring median wind speeds over the western US plains. Scientists at Blue Hill Meteorological Observatory, an isolated site south of Boston, have utilized a contacting anemometer to record wind speeds since the 1960s and have observation archives extending back to 1885 (Iacono, 2009). Iacono (2009) observed negative trends of -0.008 $ms^{-1}a^{-1}$ from 1885-2009 and -0.026 $ms^{-1}a^{-1}$ from 1960-2009. It was suggested that wind speeds at TF Green airport in Rhode Island have stilled, but a trend was not quantified in the local climatic study (Pilson, 2008). To my knowledge, substantial negative trends in New England like those at Blue Hill have yet to be identified in the published literature. Furthermore, a comprehensive study of regional New England wind speeds is absent from the recent climate

literature.

There have been a couple of extensive studies that combined many of the individual studies previously listed, attempting to estimate and classify wind speed trends over large spatial scales. A study of near surface wind speeds over the contiguous United States reported widespread stilling of in situ winds from 1973-2000 and 1973-2005 (Pryor et al., 2009). This study utilized National Climatic Data Center (NCDC) wind speed data that were normalized to a single, standard observation anemometer height of 10m in data sets NCDC-6421 (1655 stations) and NCDC-DS3503 (193 stations) (Pryor et al., 2009). Conclusions were formed after analyzing data recorded at 0000 and 1200 UTC to avoid time of observation bias in temporal trends. The study used linear trends calculated utilizing Ordinary Linear Regression and found that consistent negative wind speed trends were exhibited across the continental United States with the largest trend magnitude in the eastern and midwestern regions. An addendum (Pryor and Ledolter, 2010) reported almost identical findings in wind speed trends utilizing temporal-autocorrelation (Pryor et al., 2009).

A recently published study was conducted on a global spatial scale in a similar manner to that of Pryor et al. (2009). The investigation compiled trend analyses from 148 publications including hundreds of sites throughout the world with each data set duration greater than 30 years (McVicar et al., 2012). The OLR technique was utilized to calculate near surface terrestrial wind speed trends; a global terrestrial trend was calculated to be -0.014ms^{-1}a^{-1}, illustrating a geographically widespread stilling wind speed phenomenon (McVicar et al., 2012).

1.2.1 Wind speed metrics utilized to identify trends

Wind speed stilling has been identified in several different wind speed metrics. Many studies, most utilizing the OLR technique, identify long-term trends in mean

wind speed with units of $ms^{-1}a^{-1}$. Studies of other wind metrics support wind speed stilling observations and assertions. Pryor et al. (2009) reported a significant decrease for the annual 50th percentile of wind speed for many sites in the continental United States. Vautard et al. (2010) reported a 5-15% decline in wind speeds over the past 30 years with a greater decrease in strong winds than in weak winds. Scientists also reported on a change in frequency of light and strong winds (Mescherskaya et al., 2006), a decrease in gusts exceeding 30m/s (Sweeney, 2000), and reduced speed of maximum daily gusts (Hewston and Dorling, 2011). The frequency of storm events at 13 sites in the Netherlands decreased about 10% per decade (Smits et al., 2005). Furthermore, storm events were shorter in duration and occurred less frequently at several stations in coastal Spain (Fuentes, 2005). Greene et al. (2012a; 2012b) observed wind speeds at 10m to estimate wind power density at 80m for wind energy assessment purposes and emphasized decreases in wind power density during winter and spring. Other scientists have also reported stilling on monthly, seasonal, annual, and interannual temporal scales. For instance, McVicar et al. (2012) measured mean monthly wind speeds and trends; they also examined annual wind speeds and trends for the continent of Australia. A significant decrease in wind speeds was observed during the warming season (classified as April through October) in 22 regional sites in Canada (Burn and Hesch, 2007). In other studies, long-term trends, interannual variability (Klink, 2002), and effects of atmospheric circulation (Klink, 2007) on wind speeds in and near Minnesota were reported. The papers emphasized reduced wind speeds in the mid-west near Minnesota and explored how and why wind speeds vary from year to year.

1.2.2 Possible stilling attributions

Recent climate literature has provided possible explanations for observed reduced wind speeds on local, regional, and global spatial scales. Current literature attributes stilling to a combination of increased surface roughness, changes in atmospheric circulation patterns, and observing anomalies.

1. An increase in surface roughness can account for 25%-60% of wind speed stilling in studies in Eurasia (Vautard et al., 2010). However, this estimate is mainly from Normalized Difference Vegetation Index (NDVI) data estimations of land use and biomass changes. Surface roughness can increase due to a number of factors:

   (a) urbanization, or the expansion of urban and suburban areas (Oke, 2002) (Guo et al., 2011)

   (b) an increase in vegetation growth due to larger atmospheric CO_2 concentrations (Donohue et al., 2009)

   (c) forestation, the replanting and regrowth of former forests (Iacono, 2009; Vautard et al., 2010)

   (d) afforestation, the growth of forests in barren land always absent of forests (Liu et al., 2008)

   (e) agriculture land use changes including the amount of cultivated land used for low and high crops, especially in areas with high crops such as corn (Wieringa et al., 2001)

2. Mesoscale, synoptic, and planetary scale climate change phenomena could cause apparent stilling, such as:

   (a) a change in synoptic weather patterns including less cyclonic weather,

such as storms and associated low pressure systems, and more anticyclonic circulation (Smits et al., 2005; Fuentes, 2005)

(b) retreat of jet stream poleward (Iacono, 2009)

(c) large scale climate circulation patterns such as El Niño Southern Oscillation (ENSO), Arctic Oscillation (AO), and North Atlantic Oscillation (NAO), and associated teleconnections affecting regions differently (Klink, 2007; George and Wolfe, 2009) and changes in monsoonal patterns (Xu et al., 2006)

(d) climate change related to rapid warming of polar latitudes reducing the temperature and pressure gradients between polar latitudes and tropical and mid-latitudes (Ren, 2010)

3. Reduced wind speeds or discontinuities could be attributed to observing anomalies in some cases. Examples of observing anomalies include:

(a) the introduction of Automated Surface Observing System (ASOS) in the mid to late 1990s (McKee et al., 2000; Pryor et al., 2009)

(b) anemometer obstructions and poor site maintenance (Wan et al., 2009)

(c) anemometer height and location changes (Wan et al., 2009; Pryor and Ledolter, 2010)

(d) anemometer type and calibration changes (Wan et al., 2009; Thomas and Swail, 2011)

(e) absence of documentation for any of the items in this section (Klink, 2002; McVicar et al., 2012)

1.3 Spatial wind speed trends

Increasing wind speeds

Not all studies point to wind speed stilling. Even though many current publications indicate stilling on varying spatial scales, there are documented cases of increased wind speeds. Scientists in the State of Veracruz, Mexico observed elevated wind speeds at 5 sites with a trend of $+0.017 \text{ms}^{-1}\text{a}^{-1}$ (Cancino-Solorzano and Xiberta-Bernat, 2009). A mean trend of $+0.017 \text{ms}^{-1}\text{a}^{-1}$ was recorded at 8 sites over a period of 29 years in Spain (Recio et al., 2009), and Moratiel et al. (2011) observed a wind speed trend of $+0.040 \text{ms}^{-1}\text{a}^{-1}$ at a coastal site in Spain. Elevated wind speeds were indicated in various wind speed metric studies along with an increase in wind speed gusts (Kruger et al., 2010) and 10 minute means exceeding 20ms^{-1} and 30ms^{-1} (Fujii, 2007). McVicar et al. (2012) reported that cyclonic weather patterns, especially those associated with sub-synoptic scale fronts and storms are responsible for increases in gusts.

Apart from these isolated cases of increased wind speeds over land, there have been multiple studies that document increasing wind speed observations over the ocean. Perhaps the most well known of these manuscripts is the paper by Young et al. (2011) that recently appeared in Science. Young et al. (2011) utilized 23 years of ocean satellite altimeter data to calculate wind speeds and surface gravity wave significant heights. They reported positive trends for both variables, with higher magnitudes in wind speed trends. There was an increase in mean wind speed, but more pronounced increases were in the 90th and 99th percentiles, the latter of which indicated that extreme wind speeds over the oceans are increasing by $+0.75\%\text{a}^{-1}$. Spatially, the highest percentage increase was located in the Southern Hemisphere oceans, and the smallest trends (even negative in patches) were detected in the northern Pacific Ocean. Young et al. (2011) correlated their

results with observations from 12 deep-water buoys and concluded that although there were marked differences between buoy and satellite trends, both analyses reported similar features.

There have been other cases of increasing wind speeds over the ocean. In situ observational reports include that of Flohn and Kapala (1989), whose publication documented positive trends of $+0.014 ms^{-1}a^{-1}$ for the Atlantic and $+0.042 ms^{-1}a^{-1}$ for the Pacific. Another in situ study that utilized 5° grid cells of wind speeds measured by ships' anemometers reported an increase of $+0.020 ms^{-1}a^{-1}$ from 1982-2000 (Thomas et al., 2008) for the global oceans. Recent satellite altimetry studies like that of Young et al. (2011) concur with in situ studies, reaffirming reports of increasing near-surface wind speeds over the oceans. Tokinaga and Xie (2011) compared ship-based in situ observations to satellite measurements by constructing a data set, Wave-and Anemometer-Based Sea Surface Wind (WASWind), to homogenize in situ data. In situ data were homogenized to account for varying anemometer heights, which generally became elevated with time, and to grid data sets to monthly 4°x4°cells. They analyzed in situ data from 1950-2008 and satellite data from 1998-2008. During those time periods, Tokinaga and Xie (2011) calculated a trend of $+0.013 ms^{-1}a^{-1}$ using the satellite data and similar trends using the WASWind data. Furthermore, Wentz (2007) published an inclusive world ocean trend of $+0.008 ms^{-1}a^{-1}$ using satellite data over 1987-2006.

Global trend patterns

There have been indications of global spatial patterns in near-surface wind speed trends. Generally, terrestrial tropics and mid-latitudes have exhibited reduced wind speeds in the Northern and Southern Hemispheres; whereas increased terrestrial wind speeds have been observed at latitudes greater than 65-70° in both hemispheres. Increased wind speeds have been reported for Antarctica

(Aristidi et al., 2005; Turner et al., 2005) and Alaska (Lynch et al., 2004). As previously indicated, wind speeds over the ocean have increased.

Studies in coastal areas have documented both stilling and increased wind speeds. The complex topography and atmospheric circulation patterns such as the land-breeze/sea-breeze cycle influence near-surface wind speeds. Currently, there is not a consensus or understanding of coastal wind speed trends.

Scientists lack a complete understanding of the processes that govern the latitudinal dependence on wind speed trends. Vautard's (2010) hypothesis connecting stilling with increased surface roughness is currently the only possible justification for opposite marine and terrestrial trends at the same latitude. However, Vautard (2010) recognized that increasing surface roughness only accounted for up to 60% of stilling, and stilling has occurred during periods of negative satellite NDVI. In addition, it is very unlikely that one phenomenon could be responsible for varying wind speed trends throughout the globe; there is much to be resolved in regard to the latitudinal dependence of wind speeds and trend attribution.

1.4 Model and reanalysis data

Reanalysis data and model projections should accurately predict wind speeds trends, for inclusion in past and future climate studies. However, it has been reported on several occasions that models and reanalysis data have not accurately represented wind observations. This can cause studies to make conflicting conclusions. For instance, two research groups studied the influence of radiation, wind speed, atmospheric humidity, and air temperature on pan evaporation and evaporative trends (Matsoukas et al., 2011; McVicar et al., 2012). However, Matsoukas et al. (2011) used reanalysis data and attributed the evaporative trends to radiative changes; whereas McVicar (2012) used in situ data and attributed evaporative trends to wind speed changes.

Further research has indicated that reanalysis data and model outputs do not always represent in situ near-surface wind speed observations well. McVicar et al. (2008) demonstrated that the NCEP/NCAR, NCEP/DOE and ERA40 reanalysis data sets poorly reproduce negative wind speed trends and their spatial variability. Furthermore, additional studies in both the Northern (Smits et al., 2005) and Southern (Rayner, 2007) Hemispheres showed that observed wind speed trends have little similarity with geostrophic or model reanalysis outputs. The misrepresentation of reanalysis data is not limited to terrestrial sites: Atlantic Ocean reanalysis data trends did not agree with in situ trends calculated by Thomas et. al. in 2008 (Wever, 2012). A thorough study by Pryor et al. (2009) compared in situ and reanalysis data sets and output from Regional Climate Models (RCMs) in the contiguous United States. Their results showed that opposite (positive) trends were produced by the NARR, NCEP-1, and ERA-40 reanalysis data sets, while wide spread stilling was observed in the 50th and 90th percentiles in the in situ data sets. The Regional Spectral Model (RSM) also produced positive wind speed trends over the United States (Pryor et al., 2009). However, several studies have given favorable reports regarding model projections that correctly represented the observed wind speed trend latitudinal dependence (Yin, 2005; Seidel et al., 2008).

McVicar et al. (2008) demonstrated that reanalysis data did not exhibit similar trends as wind speed data, and recognized the importance of this flaw. They constructed continent-wide gridded cells merging in situ anemometer observations and reported decreased wind speeds for 88% of the land surface in Australia from 1975-2006. This technique was recommended for other climate variables and spatial regions as an alternative to reanalysis data for models (McVicar et al., 2008).

1.5 Motivation

Decreasing terrestrial near-surface wind speeds have been observed in the last 30-50 years. Stilling has been attributed to increased surface roughness, atmospheric circulation changes, and observing anomalies; due to complications in data homogeneity and complex physical processes, many unanswered questions remain. The hypothesized latitudinal dependence on wind speed trends raises more questions, especially in areas near the coast.

Our study is necessary for several reasons. First, the study site is located in the mid-latitudes (between 40.5°N-41.9°N), where both terrestrial stilling and increased marine wind speeds have been observed. The anemometer locations are in close proximity to the coast, which have been chosen to address the opposite trends that have been observed along coastlines. Finally, a comprehensive study of New England regional wind speeds is absent from the published climate literature.

CHAPTER 2

Data

2.1 Data sources

National Climatic Data Center

The National Climatic Data Center (NCDC), an organization maintained by the National Oceanic and Atmospheric Association (NOAA), offers online tools to acquire long-term international climatic data. The site contains a plethora of data and applications, but I concentrated on hourly/sub-hourly global data using the Climate Data Online (CDO) map application. These data sets contain variables such as wind speed, wind direction, pressure, temperature, and precipitation with time steps of an hour or less.

NCDC offers about 50 variables in which to choose, and I commonly requested wind direction, wind speed, and atmospheric pressure observations. After the data request to NCDC is processed, four files are delivered: the data file with the specified variables and time range, an inventory file with number of observations per month over the requested time range, a comprehensive header which details many quality and identification codes, and site-specific station information like the elevation, latitude and longitude.

The data retrieved from the NCDC CDO tool require formatting and manipulation before analysis in a program such as Matlab or Windographer. Oftentimes the data is recorded at irregular time intervals or has multiple observations at one single time. Also, the data can contain repeated column characters indicating the site name and wind observation type. Furthermore, a 'Q' and 'I' are listed for each individual observation. I commonly used a Unix Stream EDitor (SED) script with substitution commands to simplify the data sets into a usable form. Further

analysis is then used to organize the data into specially formatted files; these files are tailored to fit the analysis I desire, whether I am utilizing hourly, daily, or monthly wind vectors.

Very little supplementary material is available on anemometer type, height, calibration, and station location changes. The comprehensive header file contains keys to quality, type, and identification codes, but often codes are obscure. The details of observations, specifically if an "hourly" observation is an hourly mean or a single observation, are unknown until the installation of Automated Surface Observing System (ASOS) at each site, after which observations are 2-minute averages reported hourly. ASOS was generally deployed between 1993-1998 (Pryor et al., 2009). As the name states, observations by the ASOS firmware are automated, and the installation changed several characteristics of recorded wind observations (McKee et al., 2000). For instance, after ASOS was implemented, the frequency of observations of the weakest and strongest wind speeds increased. In particular, calm winds were reported more frequently, and NCDC cautions the analysis of extreme and low wind speeds (Groisman, 2002). Before ASOS was implemented, wind data was coded and reported in a teletype as 'DDFF' for a 2-digit azimuth (DD) and speed (FF). Therefore, azimuthal data were recorded with 10 degree precision, and wind speeds were documented in a whole knots (KT). Historical and post-ASOS wind speed observations are converted to m/s (1KT=0.514m/s). ASOS observations are coded with the same precision as historical measurements, or to 10 degrees and 1KT and the anemometer and wind vane starting threshold is 2KTS (Nadolski, 1998).

Although the installation of ASOS firmware altered the frequency of documented extreme and calm winds, the mean and other wind speed percentiles were not affected (Pryor et al., 2009). Pryor et al. (2009) conducted a study to iden-

tify discontinuities in the mean and 50th and 90th percentile annual wind speed values at 193 NCDC sites. Discontinuities were distributed randomly throughout all observation periods, thus confirming that the introduction of ASOS did not cause an all-inclusive disruption in wind speed metrics at United States study sites (Pryor et al., 2009).

National Buoy Data Center

The National Data Buoy Center (NDBC) is another organization provided by NOAA which offers online resources of long-term oceanographic data. NDBC is responsible for disseminating data and site information for buoys located throughout the world in oceans, seas, bays, and lakes. Buoy data sets commonly contain both meteorological variables such as wind speed and direction as well as ocean and wave characteristics.

Our interest is in historical buoy data files, which are downloaded individually by years. In addition to standard meteorological data, NDBC offers numerous variables: wave density, direction, period, and significant height. I requested standard meteorological data, and files can be downloaded immediately upon request in .txt format. Unlike NCDC files, very little is required to manipulate data files into a usable format, because data are recorded at evenly spaced intervals and files do not contain extraneous characters. However, I formatted data for its use in additional analyses.

NDBC observation documentation is extensive and accessible. Much of the data is recorded subhourly at 10 minute intervals, with a 10 minute acquisition period for each observation. The rest of the buoy data is reported in hourly intervals, with data collection periods of 10 minutes per hour at numbered buoys (44008 and 44011) and 2 minutes per hour at CMAN buoys (Buzzards Bay). All NDBC observations are given in degrees and m/s with the same precision of those

at NCDC sites (10 degrees and 0.5m/s). I will refer to Buzzards Bay as BUZM3 and Buoys 44008 and 44011 will be often be called B44008 and B44011.

2.2 Data characteristics

The majority of the data sets came from NCDC and are from the airport sites of Barnstable, Bridgeport, Nantucket, New Bedford, North Central (NC) State, and TF Green; 3 data sets were obtained from NDBC sites: 44008, 44011, and BUZM3. Site locations are shown in Figure 1, where NCDC airport sites are displayed as colored squares and NDBC buoy sites are indicated by colored circles. Most data sets contain more than 30 years of hourly data, beginning in the early 1970s and continuing through the present. The shortest data set is 20 years in duration and the longest data set contains observations for 39 years. As mentioned earlier, the NCDC data sets are comprised of hourly observations; in contrast, the NDBC data sets contain 10 minute averages for the majority of the data collection period and hourly averages for a subset of the time. Information on data sets utilized in this study is shown in Table 1.

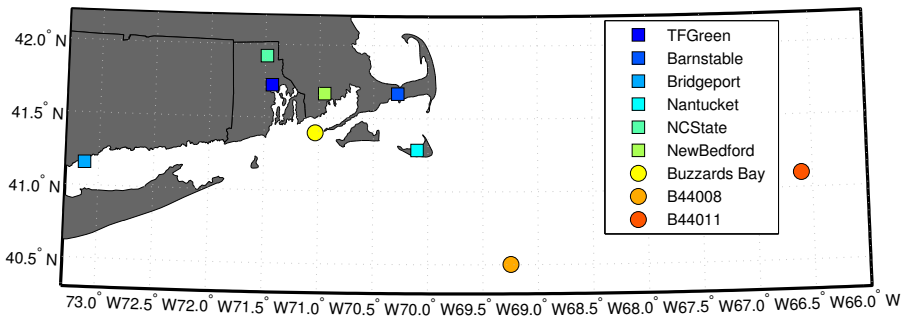

Figure 1: Study site locations, with NCDC sites shown as colored squares and NDBC buoy sites indicated as colored circles.

Gap years and/or periods with missing data are present in the data sets. For instance, there is a several-year gap in the BUZM3 data from March of 1994 until May of 1997. Many gaps, like that in the BUZM3 data, are random, but there are

systematic gaps in data at 3 NCDC airport sites: Bridgeport, Barnstable, and New Bedford. The repeating gaps originate with the beginning of recorded observations and do not cease until the installation of ASOS in the mid 1990s. These data sets are characterized by a 7-hour window without observations, usually from the hours of 0400-1000 UTC daily. Information on how I accounted for random and repeating gaps is found in the Methods chapter.

As mentioned earlier, very little information is known about anemometer type, height, and calibration changes of the stations in the NCDC archive. However, a subset of those stations was included in another data set, DSI-6421 (Groisman, 2002), that underwent considerable station research and data quality checks. Although the DSI-6421 data set was not obtained, the comprehensive documentation was acquired. Two of the NCDC sites in this study, Bridgeport and TF Green, were included in the DSI-6421 data set; information about anemometer height changes and ASOS installation is present and its utilization contributes to the robustness of the each sites' study herein. Documentation pertaining to anemometer height changes is especially useful because wind speeds change with elevation in the atmospheric boundary layer (ABL) and anemometer height changes were common: at Bridgeport, the anemometer height was altered 5 times during the study period. Techniques utilized to account for anemometer height adjustments are located in the Methods chapter.

Site	Period	Location	Comments
Buoy 44008	198208-201112	buoy: 40.502N, 69.247W	sub-hourly: 198811-201112 missing: 1982, 1988, 1996-7, 2001, 2005
Buoy 44011	198504-201112	buoy: 41.105N, 66.600W	sub-hourly: 199001-201112 missing: 1984, 1989, 1993, 2003, 2005, 2010-11
Barnstable, MA	197301-201112	airport	7 hour daily gap until 199703 missing: 2008
Bridgeport, CT	197301-201112	airport	7 hour daily gap until 199605 missing: none
BUZM3	198508-201112	buoy: 41.397N, 71.033W	sub-hourly: 199701-201112 missing: 1985, 1994-7
Nantucket, MA	197302-201112	airport	data complete, but in 3 overlapping files missing: 1974, 1992
New Bedford, MA	197301-201112	airport	7 hour daily gap until 199604 missing: 1981, 1982
North Central State, RI	199202-201112	airport	missing: 1992
TF Green, RI	197501-201112	airport	missing: none

Table 1: Onshore and offshore locations of long-term near surface wind observation sites and data record period (YYYYMM) utilized in this study. Data sets are obtained from the National Climatic Data Center (NCDC) and the National Data Buoy Center (NDBC). Years are denoted missing and are not utilized in data analysis if missing days exceed 1/3 of a year.

CHAPTER 3

Methods

3.1 Accounting for missing data

In every data set utilized in this study, data are missing in a number of instances. Missing data can be caused by a mechanical breakdown in the anemometer or an electronic malfunction in the data logger. There can also be systematic missing data from some airport sites prior to the ASOS firmware installation, when observations were only taken during flight operation hours. Furthermore, data such as an azimuth indicated as '999' and speed as '99.9' are present in many data sets. Before any data analysis, flagged data must be removed and missing data must be accounted for to avoid the introduction of a bias or artifact in the data. Complex techniques can be utilized to fill data sets or interpolate over missing values, but the methods are usually computationally involved and can introduce a bias; thus no measures have been taken to fill gaps.

It has been shown that irregular data coverage, such as partial data years, may influence annual means by introducing a bias in the estimates (Kondrashov and Ghil, 2006). Therefore, careful quality control has been performed for all data sets. Since both random and recurrent missing data are present in the study data sets, each case must be considered. Random missing data may be as brief as a single interval (1 hour or ten minutes), or as prolonged as several years. I chose to quantify the quality of the data using a measure of the fractional availability of data. A day was considered valid only if it contained 12 or more hourly observations. The maximum allowable amount of missing data in a month was 10 days. Similarly, if greater than 1/3 of the days were missing in any given season, it was rejected in seasonal analyses. Furthermore, if greater than 33% of days were absent in one year, that year was flagged because estimates were not

fully representative of annual conditions. In some cases, the year was indicated differently in a figure; in other cases the year was omitted. Pryor et al. (2009) chose similar data quality standards in their study, although the frequency of their data was at twelve hour intervals instead of hourly intervals.

Three of the study data sets, like many of the NCDC data sets, contain multiple hours of missing data each day for many years. The missing data are absent during the same hours every day; this pattern can be explained by the nature of the observation site and the exact hours that are missing. The sites with this characteristic, New Bedford, Barnstable, and Bridgeport, are all airport installations, and the missing data generally fall between 0400-1000 UTC, times when the airport was not operational. Although installation dates of ASOS are unknown for all sites, it is assumed that the recurring gaps ceased with ASOS installation because subsequently the observations are uninterrupted.

The absence of 7 hours of data per day creates a bias in the data which cannot be ignored. Until the late 1990s, the New Bedford data set is missing observations from 0400-1000 UTC (7 hours), Barnstable has no observations during the time period of 0400-0900 UTC (6 hours), and observations are absent from the Bridgeport data set from 0300-0900 UTC (7 hours). Once these time periods were calculated, all observations were removed from each data set post the ASOS deployment. Thus, a new data set was created in which each site lacked observations for about 7 hours per day throughout the entire time series. The two data sets: (1) the original data set with daily missing data until the ASOS installment and (2) the adjusted data set with missing data until the ASOS implementation and 7 hours of data withheld afterward, were then compared. Figure 2 illustrates the original data in blue and the adjusted data in red. The adjusted data is only visible after the installation of ASOS, because the values in the two data sets are identical until

then. Figure 2 illustrates that the recurrent absence of multiple hours of data per day increases the annual mean. The missing hours are generally after dusk and before dawn, when wind speeds are the weakest at most terrestrial sites; diel wind speed studies of these sites after ASOS implementation revealed these patterns. Speeds drop at coastal sites during nighttime because convective motion almost ceases, and the land-breeze/sea-breeze cycle shifts. The land-breeze/sea-breeze cycle is covered in the Results and Discussion chapter. Therefore, by removing the weakest wind speeds, the daily mean and annual mean wind speeds increase. An alteration of annual means can affect long-term trends, too. If a temporal trend was calculated with the original time series the magnitude would be much larger due to the presence of low annual means, which is an artifact of the periodic missing data.

3.2 Frequent occurrences of calms

Wind speed data at NCDC airport sites in this study are characterized by a high frequency of calms. Calms are reported at NDBC buoy sites, but are extremely infrequent and hourly averages are almost never calm. The wind azimuth associated with calms is always 999 in NCDC data, and azimuths corresponding to calms at NDBC buoy sites equal 0 or 999.

Calms or 0.0m/s wind speeds are recorded when wind speeds are less than the starting speed (or cut-in speed) of the anemometer. The starting threshold for ASOS anemometers and wind vanes is 2KT, and calms are reported when measured winds are less than 2KT (Nadolski, 1998). Wind speeds are reported as 1KT before the ASOS installation at some sites, indicating a lower cut-in speed or higher observer precision. The frequently-reported calms at airport sites include weak wind speeds in addition to calm values. A possibility to account for frequent calms is to distribute 0.0m/s wind speeds as positive values up to 2KT (the cut-in

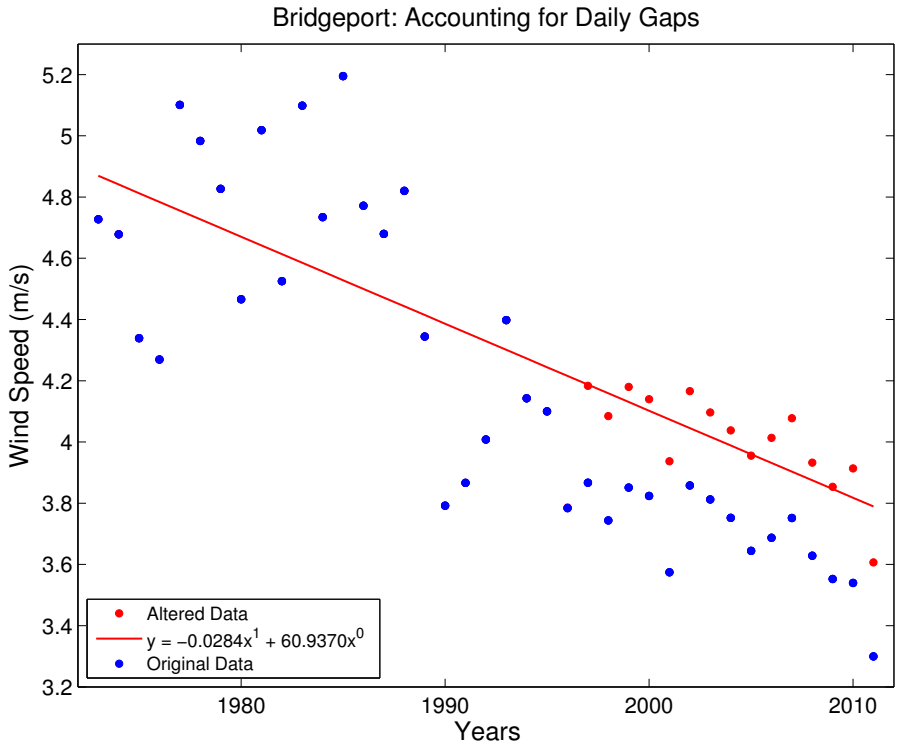

Figure 2: Time series of yearly means using two data sets at Bridgeport. The blue dots represent annual means using the original data set, in which 7 hours of data are missing until 1997. After 1997 the data is consistently recorded at hourly intervals. The red dots indicate an altered Bridgeport data set, which is exactly like the original data set (blue dots) until 1997. Post 1997, 7 hours of data have been manually removed from each day. The blue and red dots overlap until 1997. A trend line was added to the altered data (red dots). A trend would have a greater magnitude with the inclusion of the original data instead of the altered data.

speed) utilizing the Weibull Probability Density Function (PDF) as a guide. Calms would be distributed as positive values, because those are included in Weibull PDF interval. It is difficult to appropriately bin the calm values and perform the proper adjustment, especially without supporting documentation on the anemometer cut-in speed prior to ASOS installations. Furthermore, I am not absolutely certain that all calm wind speed observations are an artifact of anemometer cut-in speeds. Therefore, I have chosen to include calm wind speed observations in most calculations. Calm wind speeds are not included in Weibull parameter analyses, because

the Weibull PDF is bounded by zero, and zero is not contained in the interval.

A wind speed histogram of all winds in the data record and 45 bins at TF Green was generated, but is not shown in this document. The figure is a wind speed histogram, like Figure 11 and Figure 12, but a fitted Weibull curve is absent because only positive values are contained in the Weibull interval. The histogram that includes calm wind speeds is characterized by a bin with a very high occurrence of calm wind speeds followed by bin with a very low occurrence of weak winds just greater than 0.0m/s, and subsequently a bin with a high occurrence of wind speeds around 2m/s. Although it is not possible to fit a Weibull curve to wind data containing calm observations, the fit would be very poor.

In a time series of annually averaged wind speed percentiles for NCDC sites (not shown), the large occurrence of calm wind speeds affects annual means of 5th and 10th wind speed percentiles. Because calms are so frequent, the annual mean 5th and 10th wind speed percentiles are repeatedly 0.0m/s.

Not only do the frequent occurrences of reported calms vary between NDBC and NCDC data, but the number of calms also varies through the data record period at NCDC airport sites. Figure 3 shows the annual count of reported hourly 0.0m/s wind speeds for each year of the data record at TF Green. The annual calm counts can be described as having a large interannual variability; the annual counts range from 0 in 1991 and 1992 to 1057 in 2008, over 12% of the observations for that year. At all NCDC airport sites, the frequency of calm occurrences increases after the ASOS installation, and Figure 3 shows that TF Green is no exception. The ASOS firmware was deployed at TF Green on 01SEP1995, and this date is represented by a black vertical line in Figure 3. There is an apparent increase in reported calms after the ASOS implementation, and the annual calm totals after the installation are greater than the largest calm totals before the installation.

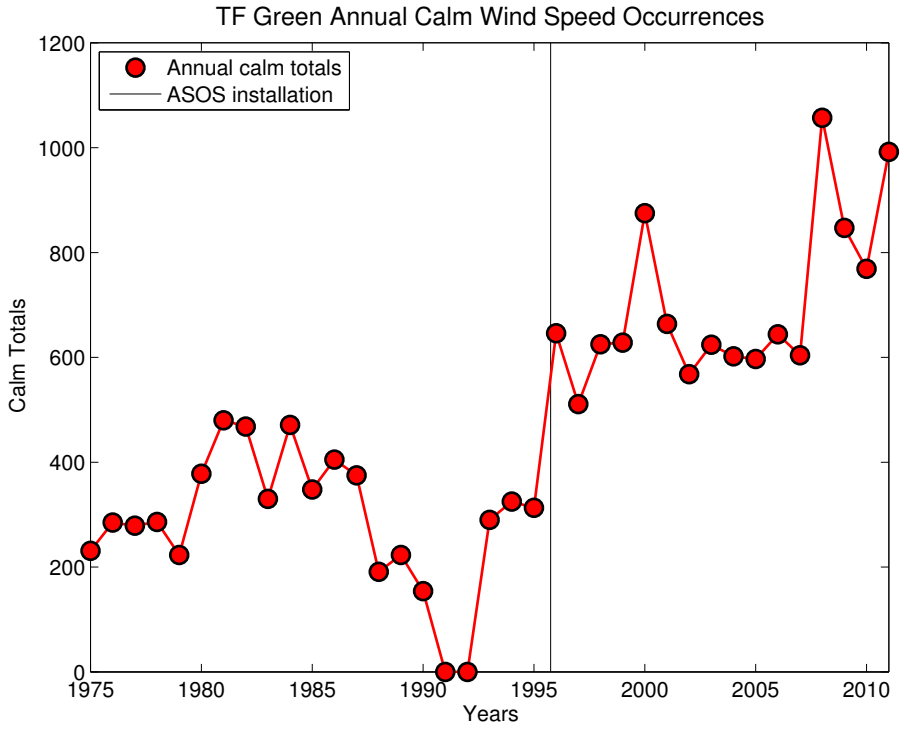

Figure 3: Time series of annual calm wind speed occurrence totals (red dots) at TF Green. A reported calm wind speed is equal to 0.0m/s. The ASOS firmware installation date at TF Green (01SEP1995) is indicated by a vertical black line.

3.3 Anemometer height homogenization

Because wind speeds increase with height in the atmospheric boundary layer, wind speeds recorded at different heights should be adjusted to a common altitude. Many studies in the current climate literature (Klink, 1999; Xu et al., 2006; Wan et al., 2009; Vautard et al., 2010) acknowledge the importance of homogenizing near-surface anemometer heights or utilize data sets in which adjustments in wind speeds have been made for anemometer height changes. The most common reference height is 10m and is recognized by the World Meteorological Organization's (WMO) Guide on the Global Observing System (GOS).

Anemometer height information is available in the DSI-6421 documentation (Groisman, 2002) for the TF Green and Bridgeport data sets. There was only one anemometer height adjustment during the study period at TF Green: on

01SEP1995 the anemometer was raised to 10m from 6.1m. Conversely, 5 adjustments were made to the Bridgeport anemometer: from 25.6m to 10.06m on 18APR1974, back to 25.6m on 15APR1976, to 24.38m on 15JUN1980, to 8.23m on 30OCT1981, and finally to 7.92m with the ASOS deployment on 01MAY1996. Anemometer heights at other NCDC airport sites have not been found. Conversely, observation information and buoy specifications are readily available for the NDBC sites. Although the anemometer heights for all three buoys in this study have not changed, none of these is at 10m. For instance, the anemometers at B44008 and B44011 are located at 5m height and Buzzard Bay buoy (BUZM3) observations are measured at 24.8m.

The logarithmic (log) law and power law are analytical representations of wind speed distribution with height. The log law is more applicable in lower, turbulent layers of the atmosphere, particularly below 30 meters height (Mikhail, 1985; Merrill and Knorr, 2012); the power law describes wind speeds over a greater height range, and has been used in the majority of studies to standardize anemometer heights. α, a dimensionless number, can be used to characterize wind speeds at elevated heights, based on surface wind speeds (Touma, 1977; Peterson and Hennessey, 1978). This relationship, given by the power law, is shown in Equation 1, where U_2 and U_1 are wind speeds at height 2 (z_2) and height 1 (z_1) respectively and α is the power law exponent or shear coefficient.

$$U_2/U_1 = (z_2/z_1)^{\alpha} \tag{1}$$

In a well-mixed ABL or neutral static stability ABL conditions, the value of α is close to 1/7 (Peterson and Hennessey, 1978; Merrill and Knorr, 2012), and an assumption of α= 1/7 can be utilized as an annual mean value (Touma, 1977; Crosby, 2011). However, ABL stability is highly variable, especially in coastal

areas; Barthelmie and Pryor (2006) showed that the land-sea boundary and coastal atmospheric processes can affect the ABL up to 20km from the shoreline. Although coastal processes and fluctuating ABL stability can introduce error with wind speed extrapolation, the assumption of α=1/7 has been used over land and sea (Peterson and Hennessey, 1978; Sedefian, 1980; Lu et al., 2002) and in the Rhode Island Sound (Grilli and Spaulding, 2010). The shear coefficient value of 1/7 was used in this study for consistency, but recent research has suggested that α=1/7 may be too high for marine wind profiles (Grilli and Spaulding, 2013). Grilli and Spaulding (2013) measured an α value of 0.086 over Block Island, offshore of Rhode Island. Even though 1/7 was utilized in this study for buoy sites, a slightly smaller α value as suggested by Grilli and Spaulding (2013) would not significantly change results.

The power law is widely applied for wind resource assessment, but it is utilized in this study to correct wind speeds with anemometer height adjustments. Corrections were applied to all data at the Bridgeport site and to the data prior to 01SEP1995 at TF Green. Wind speed corrections were also applied at BUZM3, Buoy 44008, and Buoy 44011 to adjust observations to a common anemometer height of 10m. Depending on the anemometer height change, wind speed adjustments were generally small in magnitude. For example, a wind speed of 5 m/s observed at TF Green at a height of 6.1m would be adjusted to an observation of 5.37m/s at 10m elevation.

3.4 Weibull probability density function

In many cases, the wind speed distribution can be characterized by the unimodal, two parameter Weibull probability density function (PDF) (Hennessey, 1977). The Weibull PDF has been found to closely approximate near-surface wind speed distributions (Justus et al., 1976) and

winds aloft (Baynes and Davenport, 1975). It is the most widely utilized empirical distribution (He et al., 2010) in the literature in climatic surface wind speed studies (Yan et al., 2002; Monahan, 2006; Klink, 2007; Capps and Zender, 2008) and wind power assessment (Hennessey, 1977; Lu et al., 2002; Pryor and Barthelmie, 2009).

The Weibull curve fits the asymmetrical or long-tailed distribution of wind speeds, because both are bounded by zero and positively skewed. Fits of PDFs with asymmetrical distributions have also been examined. For example, Morgan et al. (2011) evaluated 14 PDFs from 178 offshore sites which ranged from 1 to 20 years in duration. The performance of the PDFs was assessed with three metrics, including a wind speed probability plot R^2. Morgan et al. (2011) demonstrated that different distributions more accurately estimated some metrics at individual sites, but it was concluded that the Bimodal Weibull (BIW), Kappa (KAP) and Wakeby (WAK) PDFs offered the best fit for offshore wind speeds among all the study sites and metrics. However, they indicated that the BIW, KAP, and WAK PDFs were extremely complex and the PDF that offered the best fit among simpler distributions for offshore wind speeds was the Weibull (Morgan et al., 2011).

The Weibull distribution is also known as a Fisher-Tippett Type III distribution, which is a type of Generalized Extreme Value (GEV) distribution. GEV distributions are useful in representing unusually small or large observation magnitudes. The GEV is covered under the Extremal Types Theorem, in which extreme observation values of a fixed distribution will converge in a known distribution as the number of extreme observations increases. The Extremal Types Theorem in analogous to the Central Limit Theorem applied for a symmetrical Gaussian curve. Three parameters characterize GEV distributions: location or shift ζ, scale c, and shape κ. There are three classifications of GEV distributions depending

on the magnitude of the shape parameter κ. The Weibull, or the Fisher-Tippett Type III distribution occurs when ζ=0 and $\kappa < 0$ (Wilks, 2011). A separate shape parameter k and the scale parameter c characterize the form of the Weibull PDF: k describes the peakedness and width, and c is a measure of the central tendency (Pryor and Barthelmie, 2009). k is a function of the skewness and kurtosis of the distribution, and the mean wind speed and standard deviation determine c (Capps and Zender, 2008). The Weibull PDF is described by Equation 2, where *p(U)* is the PDF, k is the shape parameter, c is the scale parameter, and U are wind speed observations.

$$p(U) = (k/c)(U/c)^{(k-1)}\exp[-(U/c)^k] \qquad \text{where } U, k, c > 0 \tag{2}$$

The Rayleigh distribution, a special case of the Weibull distribution, is assumed when k equals 2. The Weibull distribution is generally characterized by $k < 3.6$, with a positively skewed curve. When k approximately equals 3.6, the Weibull PDF resembles a Gaussian curve, and if k exceeds 3.6 the Weibull curve can be described by negative skewness and will no longer have a long tail (Wilks, 2011).

Data sets were analyzed utilizing qualitative and quantitative Weibull PDF goodness of fit measures, and the maximum likelihood estimates of the Weibull parameters were computed at a 90% confidence level. In addition, the spatial variation of shape and scale parameters and analyses results of long-term and seasonal temporal variation are reported herein.

3.5 Ordinary Linear Regression

Forecasting and climate analyses often involve Ordinary Linear Regression (OLR), also referred to as linear, least-squares regression or simple linear regression. When OLR is utilized for estimation or prediction, the OLR line is referred to as a trend line. The overwhelming majority of current near-surface wind speed

climatological studies utilize the OLR method to analyze long term trends. The OLR technique is utilized to summarize a linear relationship between two variables, X and Y, where X is generally referred to as the independent or predictor variable and Y is the dependent or predictand variable. To demonstrate the linear relationship, a line of best fit, or least-squares line, of Y on X is estimated. The line is referred to as linear because it is characterized by a polynomial of the first degree and can be represented by Equation 3, where X and Y are the independent and dependent variables referred to above, and a and b are the y-intercept and slope respectively. When the OLR method is utilized, the slope b is of the same form as the Pearson Correlation Coefficient (Wilks, 2011).

$$Y = a + bX \tag{3}$$

Least squares

The line of best fit used to represent the relationship between X and Y is calculated utilizing the least squares technique. This method measures the difference between the expected and actual value of each Y at each corresponding X, which will be represented as X_i and Y_i. For instance, consider one data pair (X_1,Y_1), where Y_1 lies some distance above the best fit line. The position on the best fit line that corresponds with X_1 will be called Y; in this case, $Y_1 > Y$ and the difference Y_1- Y is denoted as d_1. This difference d_1 is also called a deviation error or a residual. There is a deviation error for each pair (X_i,Y_i) which can be positive if Y_i lies above the line of best fit, negative if Y_i lies below, and zero if Y_i $= Y$. The goodness of fit is determined by summing the residual d_i squares of all n data points: the line with $d_1^2 + d_2^2 + d_3^2 + ...d_n^2$ a minimum is considered the best fit line. Therefore, the sign of d_i is not important because each deviation error is squared. It should also be acknowledged that the mean of residuals of the best fit line equals zero (Wilks, 2011).

Confidence limits

Confidence limits, or fiducial limits, can be calculated for the y-intercept a and the slope b. These limits are the end numbers for intervals containing a certain percentage of data. For a data set statistic S (in this case S is a and b) and standard deviation σ_S, the 90% confidence interval is represented by $S \pm 1.645\sigma_S$, where 90% is the confidence level and 1.645 is the confidence coefficient or critical value (Spiegel and Stephens, 2011). The methods used to calculate confidence limits associated with the a and b in OLR are distribution-free.

3.6 Autocorrelation

Persistence refers to the characteristic of a data set which is statistically dependent on its past or future values. A data set exhibits positive statistical, or serial, dependence on its values if small values are generally followed by small values and a similar pattern with large values. This serial dependence is present in data because the time scale of the associated physical processes is as long or longer than the observation interval. Persistence is common in climatology and meteorology because of the nature of observations and their dependence on time. For instance, wind speeds, precipitation, temperature, and pressure all exhibit persistence, and all occur over varying periods of time from a brief microscale event to a several-day synoptic event (Wilks, 2011).

Data that exhibit meteorological persistence are statistically autocorrelated because no observation is independent of the previous observation. An autocorrelated data set typically has subset averages that deviate from the mean, resulting in a larger time averaged variance than a statistically independent data set with the same mean (Wilks, 2011). Furthermore, a repeated or periodic signal can be a characteristic of autocorrelated data. The presence of autocorrelation in data can foster artifacts or biases in the data, because each sample is statistically dependent

on the previous sample.

Because the wind speed data I study exists in a time series, it is temporally autocorrelated. The data consists of either 10-minute averages, hourly averages, or hourly observations, which are much shorter than many meteorological events. Although it is advantageous to resolve wind speeds 6 times per hour, observations that lie closer together exhibit a higher degree of autocorrelation. Ignoring autocorrelation in wind speed data can possibly cause inflated correlation and long-term trend estimates and smaller confidence intervals. Many wind speed climatological studies acknowledge autocorrelation but do not account for it in reported long-term trends. However, Pryor et al. (2009) acknowledged the inherent autocorrelation in their continental United States wind speed study and followed up with an addendum (2010) that focused solely on adjusting trends and confidence intervals to account for autocorrelation. Although the number of trends deemed statistically significant was slightly reduced with consideration of autocorrelation, the trend magnitudes were consistent with those when autocorrelation was not treated (Pryor and Ledolter, 2010).

There are several methods to estimate autocorrelation and its ramification in data set parameters. Equation 4 shows the effective sample size n' of a data set, where n is the number of observations in the data set and ρ_1 is the lag-1 autocorrelation coefficient (Wilks, 2011). Thus, when the data are autocorrelated, the effective sample size is reduced and can be adjusted. When no autocorrelation is present, $\rho_1 = 0$, and $n' = n$.

$$n' \cong n(1 - \rho_1)/(1 + \rho_1) \tag{4}$$

Autocorrelation was evaluated at a terrestrial and a marine site to estimate the degree of autocorrelation in the study data. The sites were evaluated from 2009-2011, a period of 3 years, utilizing hourly data from TF Green and hourly

mean data from BUZM3 at 0000 and 1200 UTC. These three years and 0000 and 1200 observations were chosen because missing data were sparse, and the continuity of observations is needed to assess autocorrelation. An autocorrelation test cannot be performed if data are absent; linear interpolation was utilized to fill missing data, which were about 1 per year. Figure 4 and Figure 5 show autocorrelation at two sites for the three year time series and the first 6 days of the autocorrelation. The 95% confidence intervals, or the critical autocorrelation lines, are indicated in red and given by Equation 5, where R_n is the critical autocorrelation value for each lag n in a data set size N (Glover et al., 2011). Autocorrelation is significant when the magnitude of the autocorrelation coefficient R_{xx} is greater than R_n, or when the autocorrelation coefficient extends beyond the confidence limits (Glover et al., 2011).

$$R_n = 1.96/\sqrt{N - n - 3} \tag{5}$$

The autocorrelation coefficient R_{xx} value at lag-1 (12 hours) and the relationship between R_{xx} values and the critical autocorrelation lines are suggestive of the degree of autocorrelation. The R_{xx} value at lag-1 is much higher for the Buzzards Bay data at about 0.5 compared to the low R_{xx} value of TF Green at about 0.15. The autocorrelation coefficient shows periodicity, indicating a strong seasonal signature in the BUZM3 data in Figure 4; the inflection points and zero crossings are representative of the change of seasons, located about 180 days apart. The magnitude of R_{xx} exceeds that of R_n at the beginning of the time series and at the seasonal troughs and ridges, confirming that the data are non-random and highly autocorrelated. A similar seasonal pattern is shown in the TF Green data in Figure 5, but the cycle is obscured and noisy. In Figure 5, the absolute value of R_{xx} is rarely greater than that of R_n, and autocorrelation is not important. The wind

speed autocorrelation results at BUZM3 and TF Green are consistent with the results from a study by Brett and Tuller (1991). In their study, wind speeds were highly autocorrelated at sites characterized by uniform topography compared to wind speeds measured at sites with complex topography (Brett and Tuller, 1991). Similarly, the BUZM3 data, collected in Buzzards Bay in open water, exhibits high autocorrelation; whereas the TF Green data is nearly statistically independent and is measured inland with inhomogeneous surrounding topography.

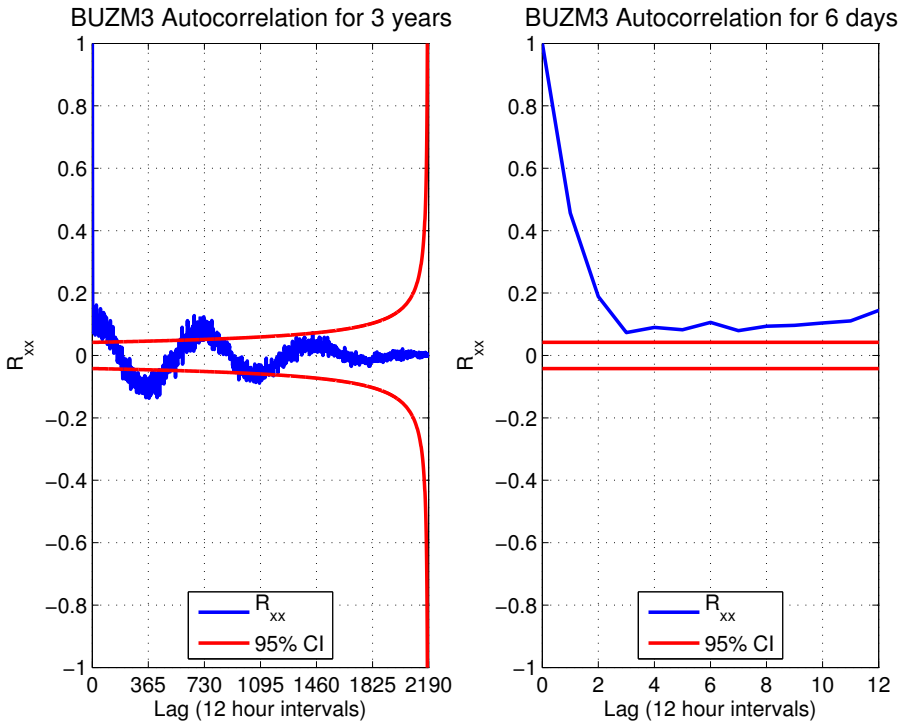

Figure 4: Temporal autocorrelation R_{xx} (blue) for three years of data at 0000 and 1200 UTC at BUZM3 (left) and first 12 lags (6 days) of the autocorrelation (right) with the 95% confidence limits indicated by the red lines calculated from Equation 5.

3.7 Resampling techniques

Unlike parametric tests, nonparametric, or distribution-free, tests are typically more computationally intensive and do not assume that the sample data and statistic are characterized by a certain parametric distribution (Wilks, 2011). Two

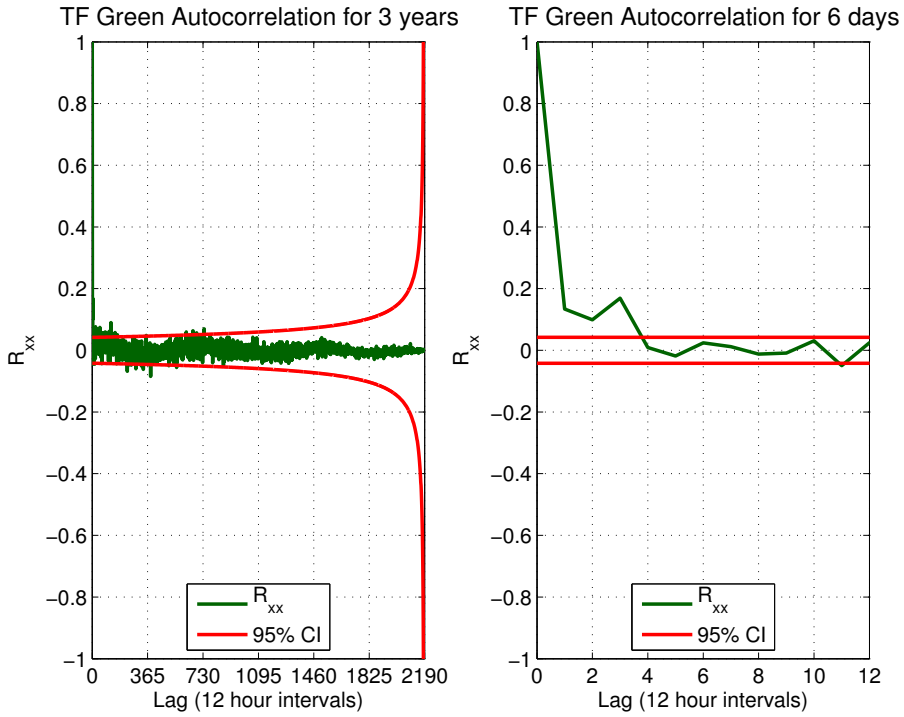

Figure 5: Temporal autocorrelation R_{xx} (green) for three years of data at 0000 and 1200 UTC at TF Green (left) and first 12 lags (6 days) of the autocorrelation (right) with the 95% confidence limits indicated by the red lines calculated from Equation 5.

types of nonparametric testing are established: the first approach focuses on data analysis utilizing parametric methods without considering the distribution, and the second technique utilizes resampling techniques to infer characteristics of the distribution using subsets of the data set. The types of nonparametric testing are known as classical procedures and resampling methods (Wilks, 2011). Nonparametric tests were used to confirm and strengthen conclusions made from parametric tests in this study.

I focus on the second type of nonparametric testing, resampling techniques, in which artificial data sets are created based on selection of points from the original data set. It is assumed that the artificial data set is representative of the original data set. Multiple artificial samples are constructed and the data set statistic and

its variance are compared. Resampling techniques are utilized to verify data set statistics calculated using parametric tests and to describe their variability and reliability (Emery and Thompson, 2001). Resampling techniques share objectives but differ in the procedures that each utilizes to generate artificial data.

Bootstrap

The bootstrap resampling method was first practiced by Bradley Efron in 1977 (Diaconis and Efron, 1983). The name originates from the expression to "pull oneself up by one's bootstraps," or to succeed without outside help; the bootstrap method is used in a single-sample setting where multiple samples are not available and therefore permutation procedures are not feasible (Emery and Thompson, 2001). Because the bootstrap is a resampling technique, it is not constrained by the assumption of a specific distribution and does not require a relation between model and statistic data properties (Emery and Thompson, 2001). Each bootstrap sample is treated similarly to the unknown distribution of the original data set. This practice is known as the plug-in principle because each sample distribution is plugged-in to estimate the original distribution of n values, where each sample has the probability $1/n$ (Wilks, 2011).

Bootstrap sampling is known as sampling with replacement, because an observation x_i, where $0 < i < n$ and i is the sample number and n is the sample size, can be present once, multiple times, or not at all in each bootstrap sample (Emery and Thompson, 2001). To construct bootstrap samples, the data are separated and placed into individual bins that correspond to random numbers. The number of bins equal the amount of data, and bins are usually assigned a random number between -1 and 1. The bin size for observations assigned to random numbers varying between -1 and 1 would be $2/n$. A sample size is usually n, but can be less than n, and random numbers between -1 and 1 are selected to fill the bootstrap

sample. With each selection, the corresponding binned datum x_i is added to the bootstrap sample and the bin is then returned to the selection pool. Thus, each bin or observation x_i can be present in a bootstrap more than once or not at all. This process is repeated for each bootstrap sample, and up to 100,000 bootstrap samples may be generated. The sample statistic is calculated for each bootstrap sample, and the statistic's true distribution can be evaluated from the bootstrap statistic frequency distribution. With a sufficient number of bootstrap samples, the statistic should exhibit convergence to its mean value (Emery and Thompson, 2001).

Jackknife

Another established resampling technique is the jackknife method, which was introduced by Maurice Quenouille in 1949 and subsequently developed by John Tukey. Tukey suggested the name "jackknife," because he likened the statistical jackknife method to an all-purpose tool (Emery and Thompson, 2001). Unlike bootstrap, the jackknife method replaces data points prior to resampling, and no repeat observations are contained in a jackknife sample. To produce a jackknife sample, a fixed number of data points are omitted from the data set. The number of deleted data points j from the total number of data points n, can range from 1 to $n/2$. The delete-1 or $j = 1$ jackknife is most commonly utilized (Emery and Thompson, 2001). In a delete-j test each jackknife sample is comprised of $S_n = n - j$ samples, with the number of deleted observations j remaining constant, but a different set of j values is removed for each sample. For example, a data set of $n = 4$ observations resampled using the jackknife delete-1 ($j = 1$) method would produce 4 jackknife samples, each of size $S_n = 3$ data points. Finally, the mean of the jackknife samples will always equal the mean of the original data set.

Resampling studies in current literature

Pryor et al. (2009) examined wind speed trends across the contiguous United States, utilizing bootstrap techniques to confirm trends were robust to the autocorrelation effects of a time series. At each site, annual mean wind speeds and percentiles were calculated from observations at 0000 UTC and 1200 UTC each day (Pryor et al., 2009). In the study, 1000 bootstrap samples were generated for each site, and regression analysis was performed for each bootstrap sample to reestimate the slope. Statistical significance of a trend at 90% confidence was indicated if trends in the middle 900 values of the frequency distribution had nonzero magnitudes (Pryor et al., 2009).

Rogers et al. (2005) utilized jackknife methods to estimate the variance and uncertainty of slopes calculated from linear regression in Measure Correlate Predict (MCP) wind techniques. They conducted multiple jackknife tests, varying delete-j to find an optimal delete-j that preserved the data distribution and ensured that each sample was independent. They showed that the jackknife variance estimate converged to the linear regression variance estimate with a large sample size if the jackknife samples were independent (Rogers et al., 2005). Because the jackknife method is not dependent on the data set parametric distribution, they were able to demonstrate that the jackknife estimate of variance correctly estimated wind speed and Weibull parameter uncertainties (Rogers et al., 2005).

In a study of $n = 20$ data points, Tichelaar and Ruff (1989) compared jackknife delete-1, jackknife delete-10 (or delete-*half*), and bootstrap methods using 100 bootstrap samples. Their objective was to compare each method's ability to estimate the reliability of a linear regression line using least squares fit. All three methods were able to produce the slope of the line accurately, but the bootstrap method's standard error of slope was lowest.

Our resampling technique

I performed regression analysis on daily mean wind speeds to estimate long-term trends for each data set. A hybrid of the bootstrap and jackknife resampling techniques was utilized to estimate the reliability of those trends. 1000 samples were generated from the original data set using resampling. Similar to bootstrap, data points x_i for each sample S_i were chosen by a random number generator; however, data were replaced after the sample was completed, not after the data point was drawn. Similar to jackknife, samples comprised a fraction of the data from the original data set; the samples S_i contained 10% of the total observations n. However, two samples could both contain similar data points, or may not contain any of the same observations. The modest sample size S_n and random filling method were chosen to minimize effects of autocorrelation in the time series. However, S_n was still large enough to preserve the original wind speed Weibull distribution and shape and scale parameters. Therefore, the sampling was representative of the population because it followed the governing distribution; yet it accounted for inherent effects of autocorrelation in the time series. The sample size S_n varied for each site, because the number of daily means differs with duration and missing data. After 1000 samples S_i were generated, the distribution was analyzed to verify convergence of the statistic mean. Similar to the analysis of Pryor et al. (2009), the slope term of the linear regression analysis was the statistic of interest, and the slopes, or trends, at a 90% confidence level were identified. I will refer to this method as Ordinary Linear Regression-Knorr Grilli (OLR-KG) after the underlying technique and those who designed it. I utilize two other techniques to estimate long-term wind speed trends. Those two techniques are the Ordinary Linear Regression-Daily Means (OLR-DM) and Ordinary Linear Regression-Annual Means (OLR-AM) and do not include resampling methods. As the names im-

ply, OLR-DM and OLR-AM both use OLR to estimate the slope term; the two methods differ in the averaging interval (daily versus yearly) of the input data.

CHAPTER 4

Results and Discussion

4.1 Local climatology and wind speed patterns

Regional winds are forced by many atmospheric physical processes and occur on mesoscale to synoptic scales. Phenomena such as the land-breeze/sea-breeze cycle, mid-latitude storms, jet stream shifts, and teleconnections of large scale climate patterns influence winds. Wind speeds at mid-latitudes are generally greater in the winter than the summer, because strong winds are characteristics of winter storms. Marine sites exhibit lower vertical shear and higher near-surface wind speeds than terrestrial sites, due to lower drag and longer unobstructed fetch. In contrast, terrestrial sites experience more shear and diel variability. Although the diel range of wind speeds is much larger at terrestrial sites, the intra-annual wind speed range at marine sites greatly exceeds that of inland sites. The large range of wind speeds on an annual time scale is evident in Figure 6, where the buoy sites BUZM3 (Buzzards Bay), B44008, and B44011, indicated by the dashed lines, exhibit an approximately 4.5m/s intra-annual speed range. The wind speed range at terrestrial sites is notably smaller, about 1m/s.

A subtle feature of Figure 6 is that the wind speed at the terrestrial sites lags that of the three buoy sites. This feature is more noticeable in the bottom panel. The speed at the buoy sites reaches a maximum value in January or February, but the terrestrial sites do not reach a maximum wind speed until March or April. The buoy site lead is noticeable in the summer months, too. Minimum speeds occur in July at most buoy sites, but speeds are weakest in August or September at terrestrial sites.

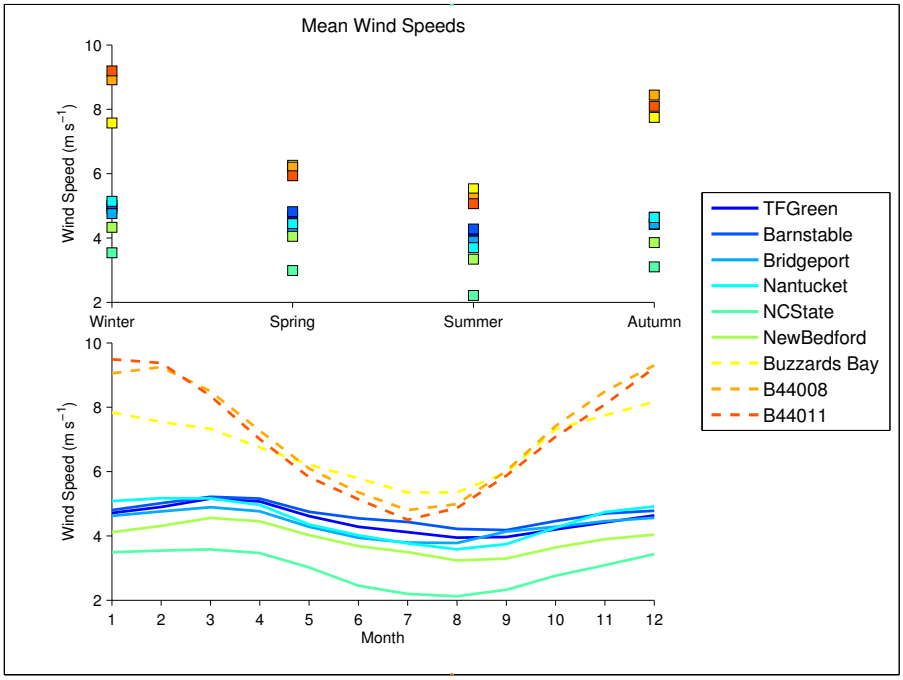

Figure 6: Categorical intra-annual wind speed variation at the nine study sites. The top panel shows seasonal mean wind speeds during the period of record for each site. Monthly mean wind speeds for the time series at each site are shown in the bottom panel. Means were calculated for individual months and seasons that contained more than 20 days and 60 days of observations respectively; months and seasons that did not meet these criteria were excluded. Winter includes January, February, and March; spring consists of April, May, and June; summer months are categorized as July, August, and September; Autumn months are October, November, and December.

Land-breeze/sea-breeze cycle

A mesoscale circulation pattern observed in many coastal areas is the land-breeze/sea-breeze cycle. This type of thermal circulation is commonly prominent year-round in the tropics and subtropics and in summer months in the mid-latitudes. The land-breeze/sea-breeze cycle is driven by the differing heating rates of the land and ocean and occurs on diel cycles and varies with seasons.

Throughout the day, the land is heated and the air above the land becomes warm; a shallow thermal low forms over the land. Concurrently, a shallow thermal high develops over the ocean, where the air is cooler. This creates a circulation cell

in which air moves from a relatively high pressure over the ocean to a relatively low pressure over the land. Air rises on land and there is return flow in winds aloft. The movement of air at the surface from the sea to land is called a sea-breeze. The sea-breeze is strongest with large temperature and pressure gradients; this occurs in the afternoon when the temperature difference between land and sea is large and near the coast where the pressure and temperature contours are tightest.

This circulation cell is reversed at nighttime when the air temperature just above the land is cooler than that above the water. A land-breeze moves from the high just above the land to the low above the water. The land-breeze is typically weaker than the sea-breeze because the temperature contrast between the land and ocean is less at nighttime.

In addition to the diel pattern of the land-breeze/sea-breeze, there are seasonal characteristics associated with its cycle in the mid-latitudes. The sea-breeze dominates in the spring and summer, when the temperature contrast between the air above the land and ocean is largest. During the winter months the air temperature is more homogeneous and the cycle is weakened.

The land-breeze/sea-breeze is evident in Southern New England regional wind speeds. The sea-breeze is strengthened throughout the day and reaches its maximum in the late afternoon. The sea-breeze is characterized by strong southerly winds near the coast in the afternoon. The magnitudes of the winds associated with the land-breeze are less and blow from the north. This mesoscale circulation pattern forces the south-southwesterly prevailing winds in the late spring and summertime, but its influence is much weaker in the wintertime.

Prevailing wind directions

The offshore Bermuda High drives anticyclonic flow and southerly winds in the summer. In addition, the south-southwesterly sea-breeze is prevalent in summer

months; wind azimuths reflect these two processes. The prevailing winds are forced by mid-latitude storms in the winter, in which strong winds blow from the north and northwest.

Wind roses in Figure 7 and Figure 8 show azimuths of daily mean data at TF Green and Buzzards Bay. Azimuth frequencies are indicated by the dotted percent circles, with the longest direction sectors corresponding to most common azimuth values. The wind roses were generated with 36 direction bins and the wind speed and azimuth frequency scales for Figure 7 and Figure 8 are identical. Colors in the legend represent daily average wind speeds in m/s that comprise each direction sector. Azimuths are plotted utilizing the meteorological convention.

The sea-breeze winds are noticeable in the southwesterly quadrant of both wind roses. In addition, the roses show strong northeasterly and northwesterly winds from mid-latitude cyclonic storms. These winds are not as frequent as the southwesterly winds, but the winds from mid-latitude storms are much stronger. A comparison of the rose in Figure 7 with that in Figure 8 reinforces the distinction between marine sites with high wind speeds and terrestrial sites exhibiting much weaker wind speeds. The sea-breeze is evident in wind roses for BUZM3 and the terrestrial sites excluding NC State, but its signature is absent from the offshore buoy B44008 and B44011 roses. Southwesterly flow is present in the wind roses at the two offshore buoys, but the substantial occurrence of southwesterly winds characteristic of other sites is not featured. The two offshore buoys and NC State are sufficiently distant from the shoreline such that sea-breeze effects are negligible.

4.2 Weibull spatial and temporal variation

Table 2 displays Weibull shape (k) and scale (c) parameters for daily mean wind speed data and corresponding 90% confidence limits. Scale parameters range from 3.35m/s at NC State to 7.96m/s at B44008. Also, k parameters span a

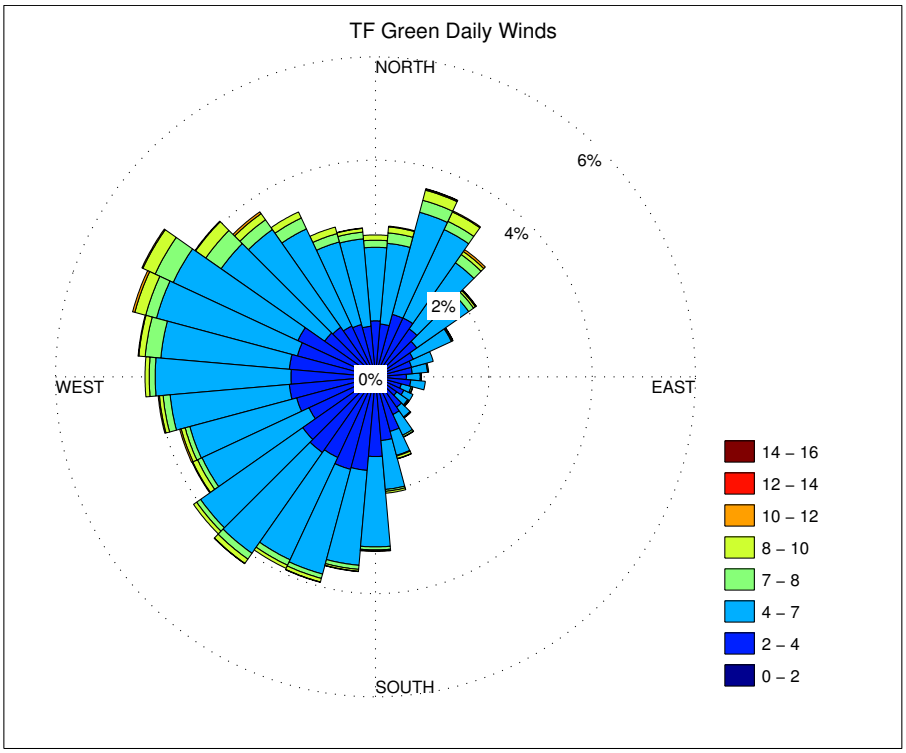

Figure 7: Daily averaged winds at TF Green over the data record period with 36 azimuth bins. Direction sector lengths are shown as percentages, indicating the frequency of daily azimuths. The wind rose is color coded by wind speeds in units of m/s that comprise each azimuth sector.

narrower range than c parameters, with minimum k of 2.16 at NC State and a maximum of 3.16 at Barnstable. As mentioned in the Methods chapter, c is a function of mean wind speed and describes the central tendency and k describes the peakedness of the distribution. Thus large c values correspond to high mean wind speeds: the largest c values are those at the buoy sites, with magnitudes that exceed 7m/s. The 90% confidence intervals are dependent on the variation and number of observations. 90% confidence limits were utilized in this study and in similar studies by Pryor et al. (2009), Young et al. (2011), and Tokinaga and Xie (2010).

Figure 9 is another way to show the relationship among Weibull parameters for sites. The y-axis is the dimensionless shape parameter k and the x-axis is

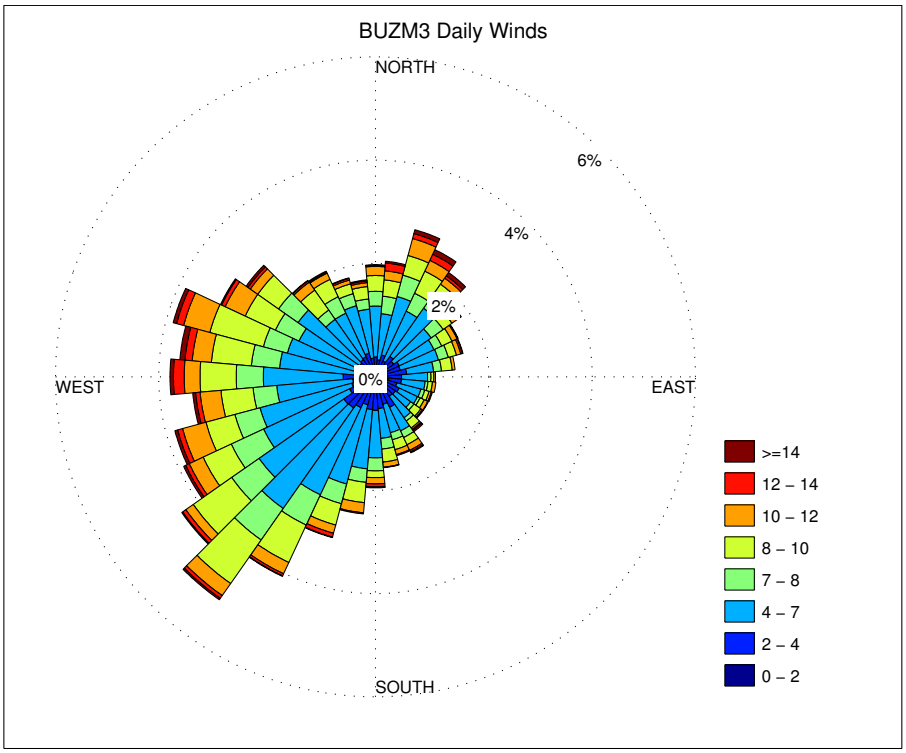

Figure 8: Daily averaged winds at Buzzards Bay over the data record period with 36 azimuth bins. Direction sector lengths are shown as percentages, indicating the frequency of daily azimuths. The wind rose is color coded by wind speeds in units of m/s that comprise each azimuth sector.

the scale parameter c. The red contours are lines of constant mean wind speed, ranging from 1m/s to 10m/s. NDBC buoy sites are represented by colored circles and NCDC airport sites are indicated by colored squares; each is plotted according to its respective k and c values.

The large range of c values between sites is evident from Figure 9 once the axes scale has been noted: the range on the x-axis is more than twice that on the y-axis. The shape parameter values have a narrow range from about 2.16 to 3.16, and the wind speed contours are characterized with little curvature above k values of 1.5. Because c describes wind speed and has a greater site to site variability than k, c will be the focus here.

The colored circle buoy sites are grouped closely together. As mentioned

above, the largest c values are observed at the buoy sites. The largest values are those of B44008 and B44011 sites, whose markers overlap. This is expected because both buoys are located offshore in an environment free of complex topography and are influenced by similar meteorological processes. Figure 9 also shows the nearly identical shape and scale values of TF Green and Bridgeport. TF Green is located at the northwest corner of Narragansett Bay and Bridgeport lies along the north shore of the Long Island Sound. Most of the NCDC airport site c parameters are clustered in the range of 4-5m/s. However, the low value of the Weibull scale parameter of NC State distinguishes the site from the other airport sites. NC State is located further inland, where wind speeds are slowed by complex topography and are characterized by a weak sea-breeze cycle.

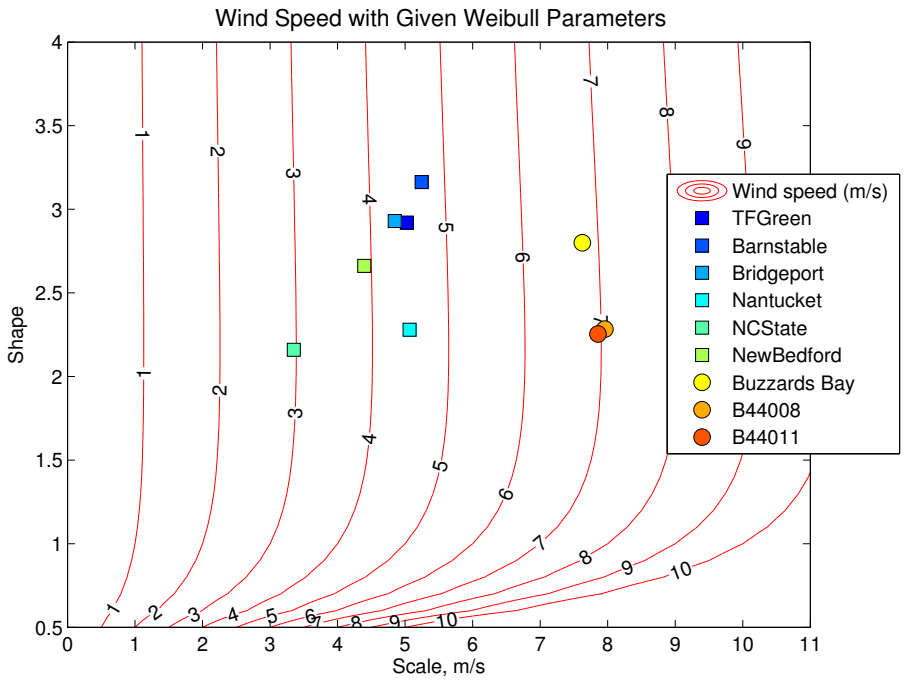

Figure 9: Wind speed contours (m/s) in red in Weibull parameter space, with k on the y-axis and c in m/s on the x-axis. Daily averaged parameters at airport sites are represented by colored squares and parameters from buoy sites are shown as colored circles. The k and c values for all sites are listed in Table 2.

Study site Weibull PDFs are shown in Figure 10; PDFs were generated using

the Weibull c and k values listed in Table 2. The PDFs for the airport sites TF Green, Barnstable, Bridgeport, and New Bedford are similar in form. Similarly, the PDFs that describe the B44008 and B44011 data overlap. Buoy site curves are notably long-tailed.

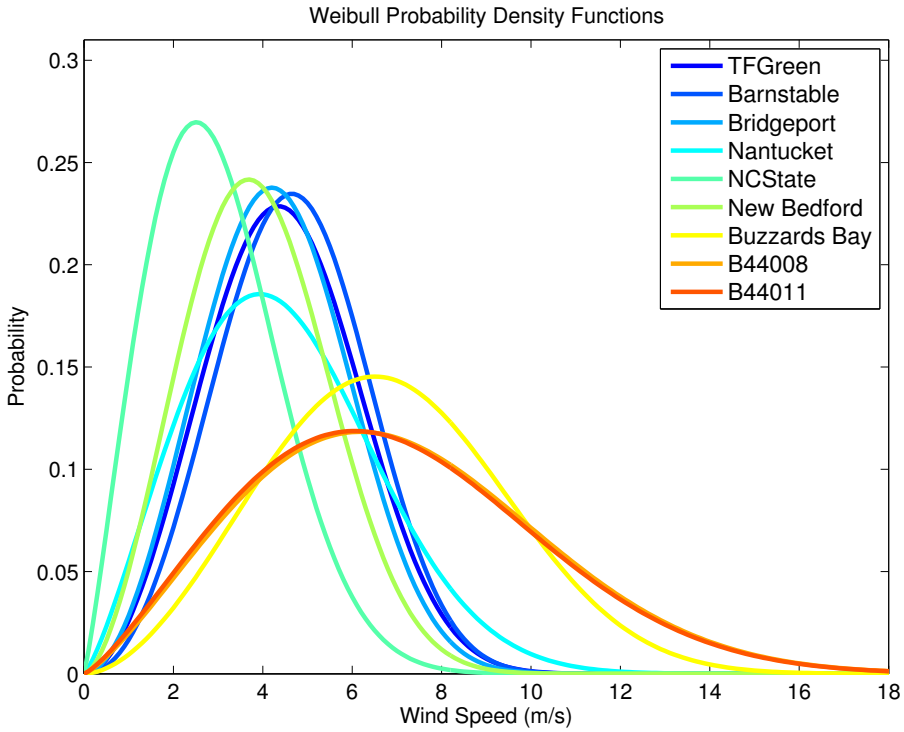

Figure 10: Weibull PDFs for study sites with occurrence displayed on the y-axis and wind speed (m/s) on the x-axis. The k and c values for all sites are listed in Table 2.

Wind speed histograms and Weibull PDFs for the TF Green terrestrial site and the B44011 marine site are shown in Figure 11 and Figure 12. To ensure equal amounts of data were represented, both figures were constructed utilizing concurrent data from 1985-2011. In addition, data were divided into 45 equally spaced wind speed bins to generate the histograms. The y-axes are occurrence, or the number of observations during the time period, and the x-axes are wind speed in m/s. Hourly mean data from 6 observations per hour are shown in Figure 12, and hourly data are shown in Figure 11. Corresponding plots made with daily-

averaged wind data have nearly identical appearance, and the corresponding c values are very similar. The daily mean c values in Table 2 and hourly c values featured in Figure 11 for TF Green differ more than those of B44011, which can be explained by the omission of 10 years of hourly data from 1975-1985. In Figure 11, the TF Green hourly wind parameter c equals 5.06m/s and the hourly mean c value at B44011 in Figure 12 is 7.83m/s. The B44011 wind speed distribution and Weibull PDF are wider than those of TF Green due to higher wind speeds, a property of an offshore buoy site. The distribution of the calm data differs between the two sites, too.

Figure 11 illustrates an absence of smooth concordance of the TF Green hourly wind speed distribution with the Weibull PDF. Very weak wind speed observations of less than about 1.5m/s are largely absent from the wind speed distribution, and the histogram shows an abrupt observation occurrence increase at about 1.5m/s. The observation occurrence exceeds that of the Weibull PDF at wind speeds from 2-4m/s and then dips below the PDF at 4.5m/s and 8.5m/s. However, from 5-8m/s and from 9-13m/s the Weibull PDF fit is acceptable. The absence of weak wind speeds may be partially explained by the excessive occurrence of calm (0.0m/s) data recorded at TF Green, where the measurement threshold is 2KTs or about 1m/s. There are a few observations below this threshold that were recorded pre-ASOS. Calms are not represented in this distribution, because zero is not included in the Weibull PDF interval. In addition to the omitted calm data, the extensive absence of agreement between the wind speed distribution and the Weibull PDF can be possibly be attributed to properties of the data coding. Another source of the disagreement might be related to the averaging period of the observations: 6 ten-minute mean wind speed observations are averaged for hourly averages in Figure 12 and hourly observations are utilized in Figure 11. As acknowledged

in the Data chapter, the averaging interval for the majority of the NDBC buoy observations is a 10-minute acquisition period and 6 10-minute averages constitute every hour; whereas observations at NCDC sites after ASOS firmware deployment include a 2-minute averaging period for each hour observation. Therefore, hourly observations at an NCDC site are characterized by large variability and much of that variability has been smoothed by averaging in NDBC site hourly mean data.

Weibull probability plots that correspond to Figure 11 and Figure 12 are shown in Appendix B. Probability plots illustrate the Weibull goodness of fit and are shown on a log-log scale with probability on the y-axis and wind speed (m/s) on the x-axis. In an ideal fit, data would lie on the straight Weibull probability line without deviations. Figure B.2 shows the Weibull goodness of fit at B44011, which is characterized by a smooth fit and low error except at very low wind speeds near the cut-in speed. The Weibull fit for the TF Green hourly mean data is poorer than that of B44011 data. An ideal fit would be linear, but extreme low and high wind speed data fall below the probability curve, with the most drastic overshoot of the Weibull plot at low wind speed values. The data coding practice introduces the artificial steps of 0.5m/s in low wind speeds.

The substantial seasonal variation at B44011 is shown in wind speed distributions for each season in Figure 13. Mean hourly wind speed distributions and corresponding Weibull PDFs for winter, spring, summer, and autumn with wind speed occurrence on the y-axis and wind speed in m/s on the x-axis are displayed. The hourly averaged wind speed data are taken from the entire time series at B44011 and 50 bins are utilized in each histogram. Although winter officially commences with winter solstice around December 21st, I categorized seasons based on whole months for ease of programming and analysis. The same number of hourly mean data points are shown in each wind speed histogram. Figure 6, which shows

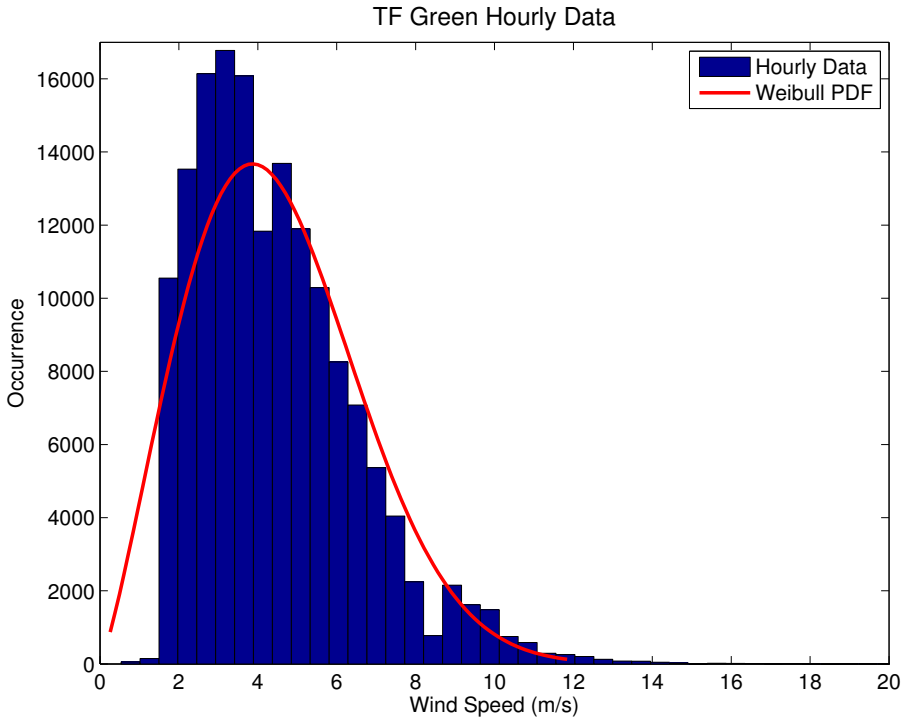

Figure 11: Hourly wind speed histogram with 45 bins (blue) and Weibull PDF (red) for TF Green data from 1985-2011. $c = 5.062$ and $k = 2.222$ for the included hourly data.

the large intra-annual mean wind speed range at buoy sites, is another way to view the wind speed variation.

The Weibull c parameter varies with each season at B44011; the mean wind speed and Weibull distribution reflect this variability. c is at its maximum value in winter at 10.2m/s, drops to 6.8m/s during spring months, falls even lower to 5.7m/s during the summer, and rises to an intermediate value of 9.1m/s during autumn. The contrast in seasonal c values at buoy sites is notable in seasonal mean wind speeds in Figure 6 and in wind speed distributions in Figure 13. The range over which relatively high occurrences of wind speeds are observed is broader for winter and autumn months, reflecting a higher central tendency and higher Weibull shape parameter values for those seasons. The peak corresponds to a lower wind speed during spring and summer and the Weibull curve is characterized by steeper slopes

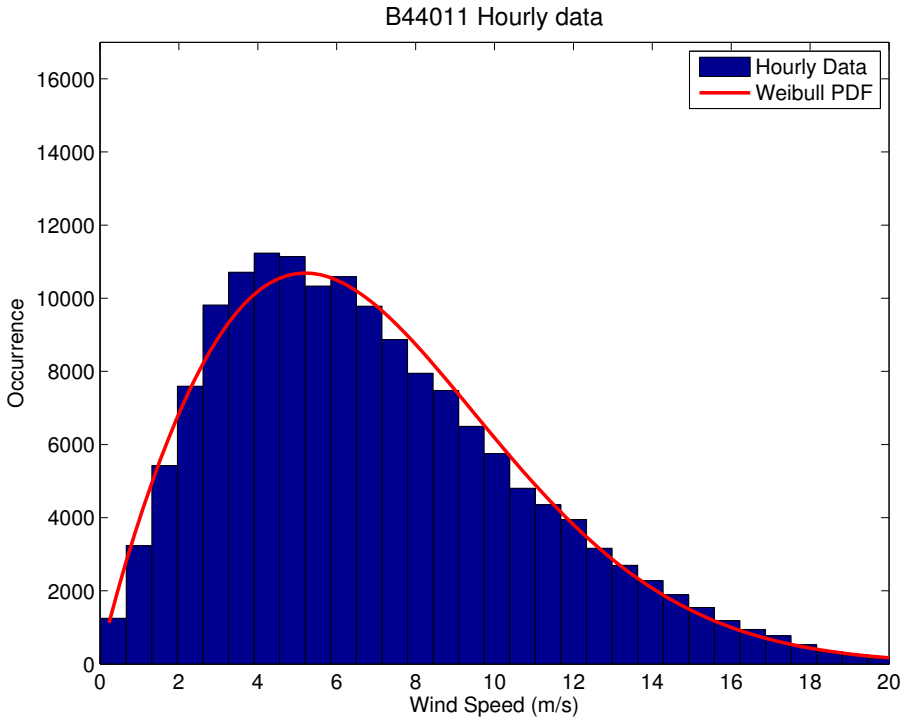

Figure 12: Hourly mean wind speed histogram with 45 bins (blue) and Weibull PDF (red) for B44011 data from entire observation period (1985-2011). $c = 7.826$ and $k = 1.872$ for the hourly mean data.

below and above its peak occurrence value. The properties of each Weibull curve in Figure 13 are expected given the location of B44011 and the regional physical processes. For instance, higher winds blow more frequently in the winter and autumn due to an increase in cyclonic weather patterns. The winds are weaker in the spring and summer months and a high frequency of low wind speeds is expected with fewer mid-latitude storms and more anticyclonic weather. However, summertime winds are still characterized by the sea-breeze at most study sites, and summertime winds at buoy sites typically have a greater magnitude than wintertime winds at terrestrial study sites.

Winds at terrestrial sites are generally characterized by low seasonal variation. The intra-annual wind speeds at TF Green are no exception and Figure 6 shows the low intra-annual range of about 1m/s. The seasonal c values for TF Green

reflect the absence of variability: the maximum c value of 5.48m/s occurs in winter, the spring c value is slightly lower at 5.08m/s, c is smallest in summer months at 4.46m/s, and the scale parameter in autumn is 5.10m/s, which is similar to the spring value. The seasonal c values are similar, but do not all fall in the confidence intervals of the other seasons. Therefore, hourly wind speed data distributions and Weibull PDFs for each season at TF Green are almost indistinguishable (not shown), although they are not statistically identical.

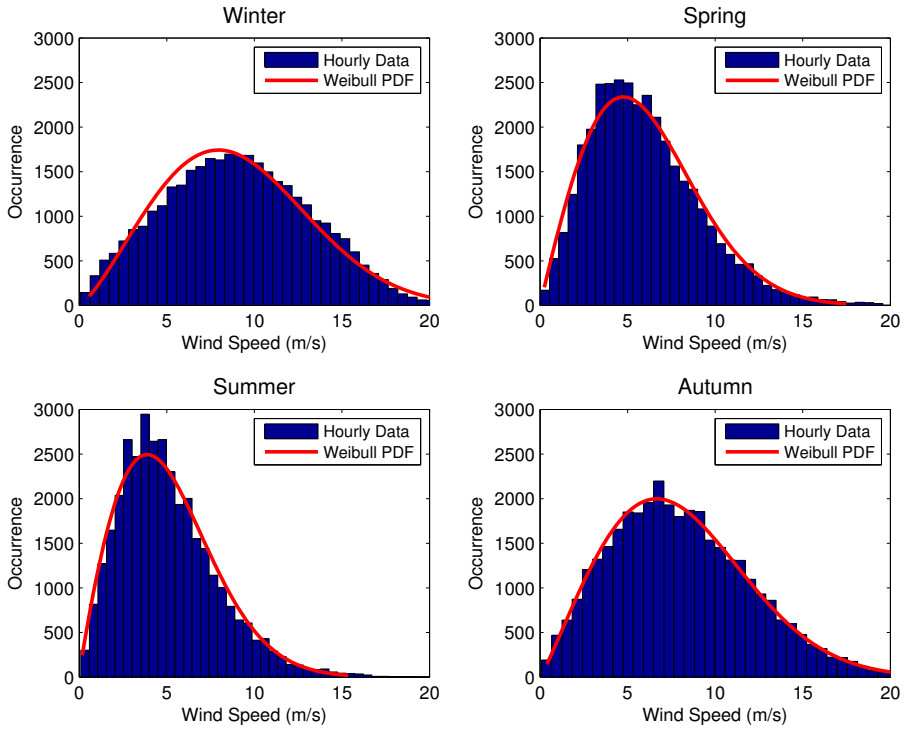

Figure 13: Wind speed histograms and Weibull PDFs for hourly means at Buoy 44011, where the x-axis is wind speed and the y-axis is occurrence. 50 wind speed bins were utilized for each histogram and data extends from 1985-2011.

4.3 Long-term mean wind speed trends

Regression analysis was applied to the data from the 9 sites and long-term trends values were inferred from the slope term. Three methods were utilized to compute long-term trends, and Ordinary Linear Regression techniques were

applied in each. The methods differ in averaging intervals and data selection. All three approaches are described in detail in the Methods section. I will refer to Ordinary Linear Regression-Daily Means method as OLR-DM; in this method, regression analysis was applied to all daily-averaged wind speed data for the time series at each site. The Ordinary Linear Regression-Knorr Grilli method will be referred to as the OLR-KG method. In OLR-KG, OLR was performed multiple times on 10% subsets of daily-averaged wind speed data. After the slope term was calculated 1000 times in OLR-KG, convergence was confirmed from its distribution and the mean value was saved. The primary objective of the OLR-KG technique was to account for autocorrelation through random resampling. The Ordinary Linear Regression-Annual Means method will be referred to as OLR-AM; in this technique, regression analysis was preformed on annually-averaged wind speeds and the slope term is analogous to the r value in the analysis. 90% confidence limits have been calculated for wind speeds from the OLR-DM and OLR-KG techniques, but confidence limits are omitted for the OLR-AM method. Confidence limits are not meaningful for annual mean trends in this study, because the annual mean data sets contain only 20-39 data points, and each data point is actually an average over multiple days. When trends from this study were tested with stricter 95% confidence limits, trend magnitudes and significance did not change.

Long-term trends and 90% confidence limits in units of $ms^{-1}a^{-1}$ calculated from the OLR-DM, OLR-KG, and OLR-AM methods are listed in Table 3. Trends and corresponding confidence intervals calculated utilizing the OLR-DM and OLR-KG methods are indicated by: *lower confidence limit*$\leq$ ***trend*** $\leq$*upper confidence limit*. Confidence intervals are consistently wider for the OLR-KG method than the OLR-DM method, because only 10% of the total daily means are utilized in each calculation. Trends are statistically significant at the 90% confidence level

if a zero trend falls outside the confidence limits. Sites that exhibit statistically significant wind speed trends at a 90% confidence level from the OLR-KG method are indicated with an asterisk in the Site column.

There are no important differences in the trend values in Table 3 between the OLR-DM, OLR-KG, and OLR-AM techniques at any site. There is an insignificant difference between trends calculated using the OLR-DM and OLR-KG methods. The largest difference is $0.0003 ms^{-1}a^{-1}$ at BUZM3 and B44008. The OLR-AM trends deviate from those calculated from the OLR-DM and OLR-KG methods, and the differences are not characterized by a pattern in magnitude or sign. The sites with the largest OLR-AM differences are NC State and B44008, in which OLR-AM trends differ from the other two methods by about $+0.0020 ms^{-1}a^{-1}$ and $-0.0015 ms^{-1}a^{-1}$ respectively. Plausible explanations for the trend magnitude discrepancies include the shorter observation record at NC State (20 years) and the numerous gap years in the B44008 data set (see Table 1). Furthermore, wind speed trends at NC State and B44008 were not significant at the 90% confidence level. Even though trend values differ between methods and confidence limits are not listed for the OLR-AM method, the OLR-AM trend values lie within the confidence limits set by the OLR-DM and OLR-KG techniques. Because additional measures were taken to account for autocorrelation in the OLR-KG method and OLR-DM and OLR-AM trends are contained in the OLR-KG confidence intervals, I will refer to the OLR-KG trend values in all further discussion.

In Table 3 and Figure 14, six of the nine study sites exhibit statistically significant long-term wind speed trends, and the trends vary in magnitude and sign. In Figure 14, statistically significant trends are indicated by colored squares, and colored diamonds represent insignificant trends; positive trends are colored red, and negative trends are shown by blue shapes. Long-term trend magni-

tudes greater than $0.03 ms^{-1}a^{-1}$ are characteristics of wind speed at Nantucket ($+0.0438 ms^{-1}a^{-1}$), TF Green ($-0.0377 ms^{-1}a^{-1}$), and B44011 ($+0.0335 ms^{-1}a^{-1}$). The smallest trend magnitude that is still classified as statistically significant is $-0.0074 ms^{-1}a^{-1}$ at New Bedford. Even though the magnitude of the trend at NC State exceeds that of New Bedford, the trend at NC State is not significant at a 90% confidence level because there are almost twice as many daily mean observations at New Bedford than at NC State. Trends also differ in sign: 4 of the 6 statistically significant trends are negative and 2 are positive.

Site	**Scale Parameter c (m/s)**	**Shape Parameter k**
TF Green	$5.00 \leq \mathbf{5.02} \leq 5.05$	$2.89 \leq \mathbf{2.92} \leq 2.95$
Barnstable	$5.22 \leq \mathbf{5.24} \leq 5.27$	$3.13 \leq \mathbf{3.16} \leq 3.20$
Bridgeport	$4.82 \leq \mathbf{4.85} \leq 4.87$	$2.90 \leq \mathbf{2.93} \leq 2.96$
Nantucket	$5.03 \leq \mathbf{5.07} \leq 5.10$	$2.26 \leq \mathbf{2.28} \leq 2.30$
NC State	$3.319 \leq \mathbf{3.35} \leq 3.39$	$2.13 \leq \mathbf{2.16} \leq 2.19$
New Bedford	$4.37 \leq \mathbf{4.40} \leq 4.42$	$2.63 \leq \mathbf{2.66} \leq 2.69$
BUZM3	$7.57 \leq \mathbf{7.62} \leq 7.68$	$2.76 \leq \mathbf{2.80} \leq 2.84$
B44008	$7.89 \leq \mathbf{7.96} \leq 8.03$	$2.25 \leq \mathbf{2.28} \leq 2.32$
B44011	$7.78 \leq \mathbf{7.86} \leq 7.93$	$2.22 \leq \mathbf{2.25} \leq 2.29$

Table 2: Weibull shape and scale parameters (in bold font) and 90% confidence intervals calculated using daily mean wind speeds.

Site	Trend (OLR-DM)	Trend (OLR-KG)	Trend (OLR-AM)
TF Green*	$-0.0398 \leq$ **-0.0378** ≤ -0.0358	$-0.0442 \leq$ **-0.0377** ≤ -0.0313	**-0.0380**
Barnstable*	$-0.0219 \leq$ **-0.0201** ≤ -0.0182	$-0.0262 \leq$ **-0.0202** ≤ -0.0142	**-0.0201**
Bridgeport*	$-0.0299 \leq$ **-0.0281** ≤ -0.0263	$-0.0337 \leq$ **-0.0280** ≤ -0.0223	**-0.0284**
Nantucket*	$+0.0411 \leq$ **+0.0436** $\leq +0.0462$	$+0.0358 \leq$ **+0.0438** $\leq +0.0518$	**+0.0453**
NC State	$+0.0047 \leq$ **+0.0100** $\leq +0.0152$	$-0.0066 \leq$ **+0.0101** $\leq +0.0268$	**+0.0123**
New Bedford*	$-0.0094 \leq$ **-0.0074** ≤ -0.0055	$-0.0135 \leq$ **-0.0074** ≤ -0.0013	**-0.0071**
BUZM3	$-0.0100 \leq$ **-0.0034** $\leq +0.0033$	$-0.0248 \leq$ **-0.0037** $\leq +0.0175$	**-0.0034**
B44008	$-0.0023 \leq$ **+0.0048** $\leq +0.0120$	$-0.0182 \leq$ **+0.0045** $\leq +0.0272$	**0.0031**
B44011*	$+0.0244 \leq$ **+0.0335** $\leq +0.0425$	$+0.0042 \leq$ **+0.0335** $\leq +0.0619$	**+0.0344**

Table 3: Long term trends in $\mathrm{ms}^{-1}\mathrm{a}^{-1}$ at sites calculated utilizing the OLR-DM method and the OLR-KG method with daily means and the OLR-AM method with annual mean wind speeds. Ninety percent confidence intervals are indicated for the OLR-DM method and the OLR-KG method and trends are listed in bold font. All trends calculated with annual mean values are within the 90% confidence limits of the trends calculated utilizing the OLR-DM method and the OLR-KG method. Asterisks indicate sites with statistically significant wind speed trends.

4.3.1 Spatial trend patterns

The spatial variation of long-term trends as reported in recent climate literature was addressed in the Introduction. Widespread negative wind speed trends have been observed in numerous areas and at multiple spatial scales, including the US Mid-West region (Klink, 2002; Greene et al., 2012b; Greene et al., 2012a), the contiguous United States (Pryor et al., 2009), Australia (Roderick et al., 2007), Europe (Wever, 2012), and the throughout the world (McVicar et al., 2012). In contrast, increasing wind speed over the world's oceans indicated by positive wind speed trends has been recorded by quality controlled ship and buoy anemometer data (Thomas et al., 2008; Tokinaga and Xie, 2011) and satellite scatterometer and altimetry (Young et al., 2011) observations. In addition, a latitudinal dependence of terrestrial wind speed trends has been suggested, with positive trends at the poles and negative trends in the tropics and mid-latitudes (McVicar et al., 2012). These reports and assertions offer general trend classifications onshore and offshore, but coastal long-term wind speed trend studies are largely absent from the published literature and patterns in long-term wind speed trends have not been identified.

The spatial trend distribution in Figure 14 generally parallels mid-latitude spatial trend patterns described in climate literature: onshore sites are described as having negative wind speed trends and wind speed at offshore sites generally exhibits positive trends. However, there are exceptions to this simple pattern in the literature and also in this study. For example, wind speeds are stilling at the offshore buoy BUZM3 and wind speeds are increasing inland at NC State. However, the trends at these two exceptional sites are not statistically significant and Figure 14 reaffirms that long-term trends in this study can be characterized as spatially coherent and not isolated.

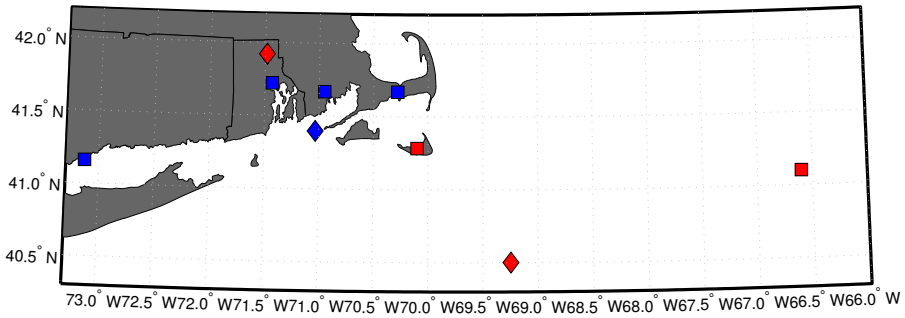

Figure 14: Long-term trends at study sites classified by statistical significance at a 90% confidence level (squares), statistically insignificant at a 90% confidence level (diamonds), positive (red), and negative (blue). Trend significance was determined from the OLR-KG method.

4.3.2 Categorical temporal trends

Trends were calculated with the OLR-DM technique for each month and season at all sites and results are displayed in Figure 15. The top panel of Figure 15 shows the trend in $ms^{-1}a^{-1}$ on the y-axis for each season on the x-axis at sites shown by colored shapes. Squares indicate a statistically significant long-term trend and the colored diamonds represent a statistically insignificant trend; the significance was determined from values in Table 3. If a particular season had more than 30 missing days, the season was excluded in the trend analysis. Monthly trends in $ms^{-1}a^{-1}$ for the time series at each site are shown in the bottom panel of Figure 15. Statistically significant trends at sites (from Table 3) are indicated by heavy weight colored lines and statistically insignificant trends are shown by thin weight colored lines (NC State, Buzzards Bay, and B44008). Months were not included in the analysis if more than 10 days were missing per month.

The motivation behind the calculations of the results presented in Figure 15 was to resolve if long-term trend values were steady throughout the year, or if a trend in certain seasons or months dominated the long-term value. Buoy site wind speed trends appear to have the largest positive values in the autumn and winter, and the largest negative values in the summer. However, trends at buoys show

large intra-annual variation, which is noticeable in the lower panel. For example, the trend ranges from 0ms^{-1}a^{-1} in June to almost +0.08ms^{-1}a^{-1} in October at B44011 and from -0.04ms^{-1}a^{-1} in June to +0.06ms^{-1}a^{-1} in October at B44008. At many terrestrial sites, especially those with significant negative trends, the trend magnitude is constant throughout most of the year.

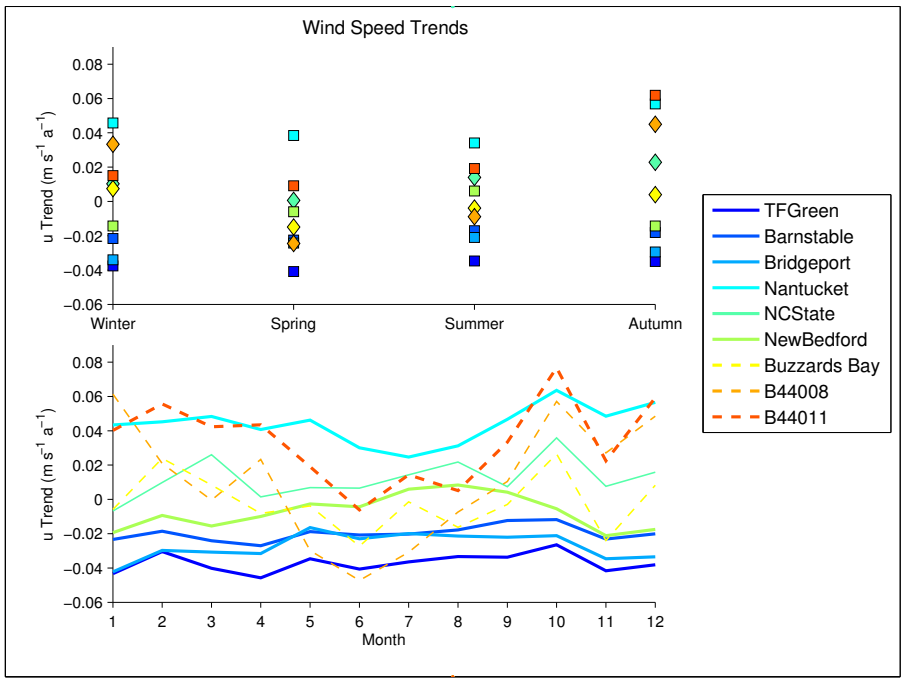

Figure 15: Seasonal (top) and monthly (bottom) wind speed trends in ms^{-1}a^{-1} at all sites. Statistically significant trends determined by the OLR-KG method from Table 3 are indicated by colored squares (top) and thick lines (bottom). Statistically insignificant trends are represented by colored diamonds (top) and thin lines (bottom). Seasonal and monthly data were excluded if a particular season or month was missing more than 1/3 of the daily means.

4.4 Long-term trends in additional metrics

Although many climatological wind speed studies examine annual mean wind speed and report trends in units of ms^{-1}a^{-1}, other metrics have been used in other wind speed studies. As mentioned in the Introduction, scientists have published metric studies including trends in extreme

weak and strong wind speeds (Mescherskaya et al., 2006; Vautard et al., 2010), storm frequency (Smits et al., 2005; Fuentes, 2005), gusts (Sweeney, 2000; Hewston and Dorling, 2011), and wind power density (Greene et al., 2012b). I analyzed two additional wind speed metrics at each site: annual mean wind speed percentiles and annual mean Weibull parameters.

4.4.1 Trends in wind speed percentiles

Pryor et al. (2009) studied long-term variation in the 5th-95th annual wind speed percentiles, and focused on the 50th (median) and 90th annual percentiles. The data they utilized were recorded twice-daily, with observations at 0000 and 1200 UTC. After analyzing wind speed from over 1000 US sites, they concluded that geographically widespread wind speed stilling was occurring in the 50th and 90th percentiles in the continental US sites (Pryor et al., 2009).

I analyzed the long-term variation of the 5th, 10th, 25th, 50th, 75th, 90th, and 95th percentiles at all study sites. Time series figures (not shown) can be described as geometric, because annual percentile values are members of the data set (not averaged), in which observations are coded with a finite precision of .5m/s.

Although none of the figures are included in this document, a few features will be described. Generally, wind speeds in the highest percentiles (90th and 95th) are consistently characterized with the largest interannual variability. In addition, if wind speeds are anomalously high or low, the anomaly pervades most or all of the percentiles of that particular year. The large occurrences of zeros at NCDC airport sites highlighted in the Methods chapter is apparent in the 5th and 10th annual mean wind speed percentiles. For instance, reported calm wind speeds are so frequent in the New Bedford and NC State data that many of the annual mean 5th and 10th percentiles in the time series are equal to 0m/s.

At Nantucket and Bridgeport, interannual wind speed percentile variability

and wind speeds appear to abruptly increase and decrease respectively without a large gap in wind speed observations. After a missing year at Barnstable, annually averaged wind speed percentiles can be described by a systematic decrease. An abrupt change in all wind speed percentiles is suggestive of a data discontinuity.

Mean wind speed trend signs are consistent with those in annual mean wind speed percentiles. Long-term percentile trend magnitudes are greatest in the smallest (5th and 10th) and largest (90th and 95th) annual wind speed percentiles.

4.4.2 Long-term variation of Weibull parameters

Other metrics utilized to measure long-term wind speed trends are the Weibull shape k and scale c parameters, and studies that examine long-term Weibull parameter variation include those of Klink (2002), Wichser and Klink (2008), and Barthelmie and Pryor (2009). In this study, annual mean k and c parameters and corresponding 90% confidence limits were calculated for wind speeds at each site. Again, I highlight the c parameter because it is a function of mean wind speed. In addition, annual k values are rarely less than 1.5, meaning that the influence on annual mean wind speed from the k parameter is almost negligible (see Figure 9). In addition, corresponding k parameter time series are generally characterized by having a zero trend or trend with a very small magnitude.

Figure 16 and 17 show a time series of annual mean c parameters and a regression line from the least squares fitting technique. 90% confidence limits are indicated for each annual mean c value, and a solid least squares fitted line shows the trend over the time series. In Figure 16, a dotted line has been added to TF Green annual c parameters from 1985-2011 to illustrate that the trend is greater after 1985 than it was before. The equations associated with the regression lines in Figures 16 and Figure 17 are listed in the legends. Included in the equations is the slope term determined from regression analysis and associated with the long-term

trend.

At all sites, c trend signs conform with those of mean wind speed trends, but the trend magnitudes are not identical. Therefore, time series of annual c parameters at each site exhibit similar features as mean wind speed trends, confirming that trends are identified in multiple wind speed metrics. The annual mean Weibull scale parameter trend value at Nantucket is $+0.0228 ms^{-1}a^{-1}$ (Figure 17); the trend calculated from annual mean wind speeds (OLR-AM method) at the same site is $+0.0453 ms^{-1}a^{-1}$. Annual mean wind speeds are characterized by a trend of $-0.0333 ms^{-1}a^{-1}$ at TF Green, and the Weibull scale parameter trend is $-0.0378 ms^{-1}a^{-1}$. The annual mean scale parameters at Nantucket, shown in Figure 17, increase throughout the time series, and the parameters are characterized by a large amount of interannual variability. In contrast, at TF Green, c values decrease from 1975-2011, and the least squares line appears to fit the data more closely.

4.4.3 Changes in wind azimuths

I analyzed daily mean azimuths at study sites in multi-year periods at the beginning and end of each data period. The goal of this analysis was to identify the presence or absence of an azimuthal shift (or lack thereof) in each time series. A change in wind direction is suggestive of a shift in weather patterns or a different upstream drag profile, both of which could influence wind speeds.

At sites with statistically significant negative trends, winds generally blew more frequently from the southwest and less frequently from the northwest at the end of the time series. In contrast, opposite patterns were observed in daily mean azimuths at sites with statistically significant positive trends. Distinct wind rose changes were observed at the Nantucket and New Bedford sites. At Nantucket, a daily mean wind rose from 2007-2011 was characterized by far fewer occurrences

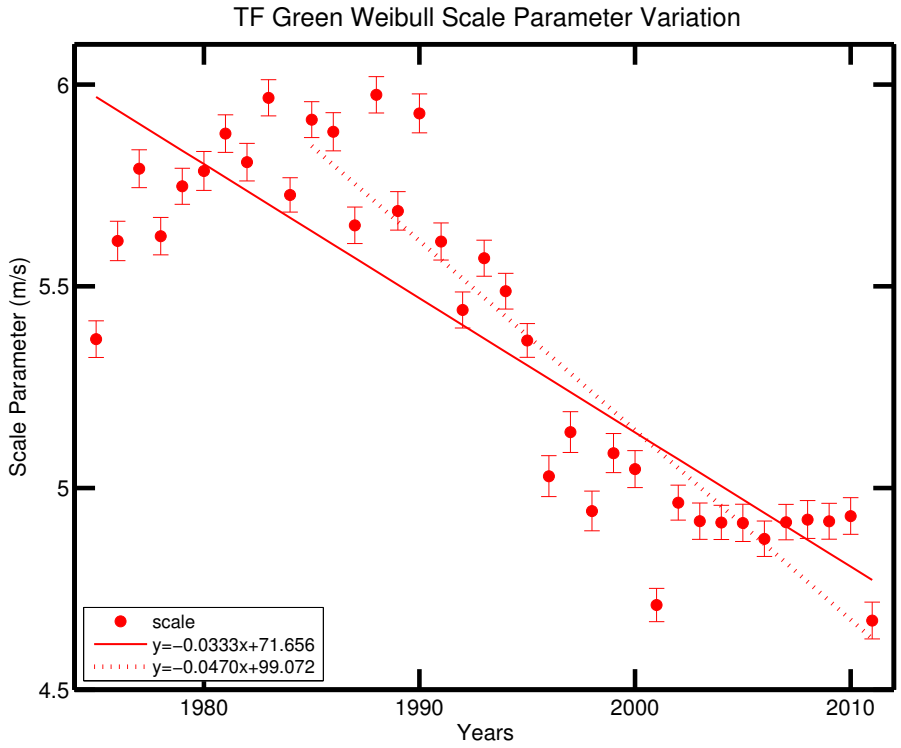

Figure 16: Time series of annual mean Weibull scale c parameter (m/s) variation with 90% confidence limits at TF Green. Regression lines from the least squares fitting technique have been added for the entire time series (solid) and 1985-2011 (dotted) and corresponding equations are shown in the legend.

of southwesterly winds than the 1975-1979 rose. In contrast, stilling winds at New Bedford experienced a marked shift in azimuths with less frequent northwesterly winds in 2007-2011 than in 1973-1977. These wind roses are not shown here, but their structure is similar to those in Figure 7 and Figure 8.

The observed alterations in wind direction are generally subtle and are not easily quantified. However, a change in the frequency of wind azimuths as reported may provide some explanation to the observed long-term wind speed trends. Higher storm frequency could force an increased amount of strong winds from the northeast and northwest, resutling in a positive wind speed trend. Conversely, a negative trend might be justified by a higher occurrence of weak southwesterly winds from anticyclonic weather.

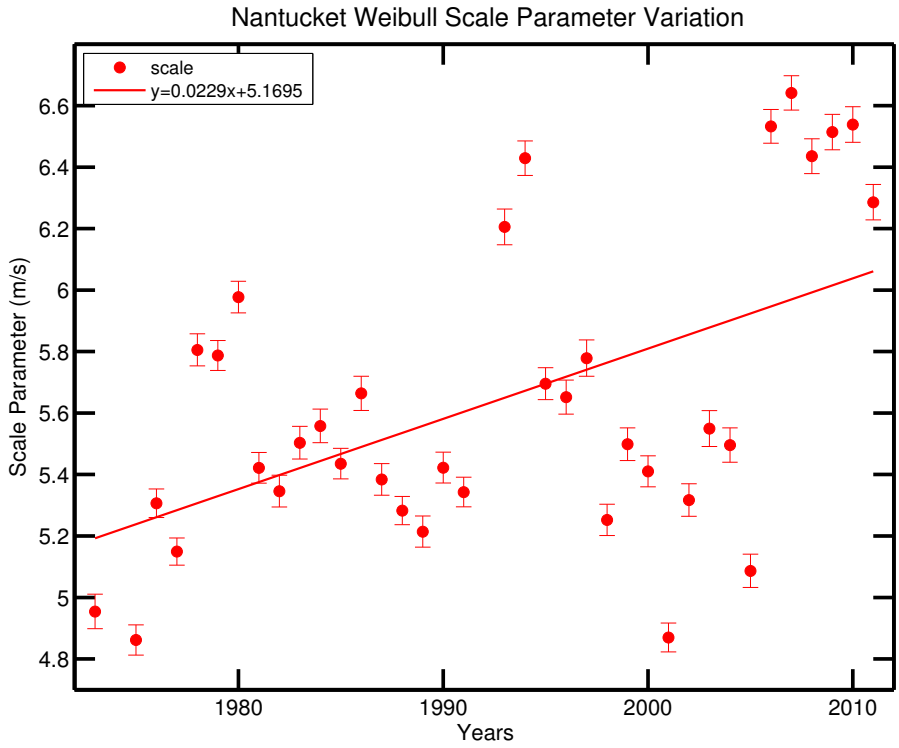

Figure 17: Time series of annual mean Weibull scale c parameter (m/s) variation with 90% confidence limits at Nantucket. A regression line from the least squares fitting technique has been added for the entire time series and its corresponding equation is shown in the legend.

4.5 Principal Component Analysis (PCA) and cluster analysis

A Principal Component Analysis (PCA) is a statistical data reduction method utilized to express a group of variables as a single new variable or to minimize the number of variables. The new variables are referred to as Principal Components (PCs), and all PCs are orthogonal to each other; therefore, no information is redundant (Emery and Thompson, 2001). The combined PCs, or statistical modes, account for all the variance in the data. Since the primary goal of the PCA analysis is to reduce the variables, a few PCs should contain a significant amount of the total variance.

Clustering techniques are utilized to separate data into groups in a multispace and analyze their relationship. I analyzed data with the k-means cluster method,

which partitions data by optimizing separation distance between exclusive clusters and minimizing inclusive cluster distance (Corti, 2012). To do this, the k-means method maximizes the ratio of the inter-cluster centroid variance to the mean intra-cluster variance, also known as the seed value (Corti, 2012).

I performed a PCA and k-means cluster analysis on TF Green and BUZM3 data to identify a change in synoptic weather from the beginning to the end of the time series. The meteorological variables used were wind speed, wind azimuth components u and v, pressure, and temperature for a five-year period at the beginning and end of the time series. However, the variables could not be reduced because the percent variance explained by all 5 PCs was around 20%, and the maximum percent variance was about 27%. Therefore, all variables and PCs were important in the analysis. There were no striking changes because the modes were statistically insignificant. The number of variables could not be reduced, so all five PCs were inputted to the cluster analysis. The cluster analysis seed value remained relatively small with a maximum around 0.38 and did not change significantly with different numbers of clusters. Therefore, the PCA and cluster analysis confirmed that the synoptic weather has remained consistent in the last 25 years at TF Green and BUZM3. The results from these tests could be fortified by an additional tests using more variables, such as precipitation, ceiling height, temperature profile, and humidity. However, the variables are limited, especially at the beginning of the time series.

4.6 Possible causes of long-term trends

Multidecadal wind speed trends can be attributed to processes internal to the climate system, to a change in surface roughness, and/or to observing anomalies. Observation analyses results have given insight to the causes of wind speed trends in Southern New England.

Figure 15 shows large positive wind speed trends in the autumn and winter and contrasting (negative or zero) trends in the spring and summer at buoy sites. These trends could be indicative of an increase in winter mid-latitude storms offshore, thus providing a possible explanation for positive offshore wind speeds in this and other studies. To my knowledge, there are no published regional studies verifying this hypothesis. Smits et al. (2005) studied temporal distributions of independent wind events (storms) in the Netherlands, and a similar study could be carried out to verify this hypothesis. Furthermore, a regional decrease in cyclonic weather might explain the observed wind speed stilling at terrestrial sites.

Discontinuities in annual mean wind speed and percentiles at several terrestrial sites (not shown) raise concerns, especially when discontinuities are paired with gap years and known anemometer height and calibration adjustments. Pryor et al. (2009) tested 193 sites in the NCDC DS-3505 data set for discontinuities with a 5-year running mean of annual 50th and 90th wind speed percentiles and concluded that discontinuities are equally distributed throughout the data record, not concentrated at the time of the ASOS deployment. However, the sites I examine were not included in this test, and wind speed discontinuities (and trends) may be influenced by anemometer height changes and ASOS firmware installations.

Even though I have no quantitative measurements of forestation and urbanization, the possibility exists that these processes could contribute to wind speed stilling at many onshore locations. Furthermore, it has been speculated that two distinct processes could be simultaneously affecting winds. For instance, a widespread process could be controlling the increase of wind speeds offshore; yet this physical process might be masked onshore by an increase in surface roughness causing stilling winds.

CHAPTER 5

Conclusions and future work

5.1 Summary

Long-term wind speed data were obtained from NCDC and NDBC at 9 coastal New England sites. Analyses revealed meteorological processes that drive regional wind speeds, which include the land-breeze/sea-breeze cycle, mid-latitude storms, and persistent high and low pressure systems. The spatial variation of Weibull parameters was studied, and I calculated larger c parameters, a wider distribution, and larger intra-annual variability offshore. Smaller c values and reduced seasonal variability describe wind speeds at onshore sites.

Wind speed trends were calculated from three regression analysis methods that differed in averaging intervals and sampling techniques. Long-term trends calculated from all three of these methods were in agreement, and coastal New England wind speed can be characterized by spatially coherent wind speed trends. Wind speed trends at six of 9 study sites are statistically significant at a 90% confidence level; 2 sites exhibit positive wind speed trends and stilling has been calculated at 4 sites. The spatial distribution of trends conforms with the general pattern of reported wind speed trends in published literature, with negative trends onshore and positive trends offshore.

Additional wind speed metric analyses of Weibull scale parameters and wind speed percentiles corroborate long-term trends. Annual Weibull scale parameters were analyzed with the OLR technique, and trend signs concurred with those of annual mean wind speed. Time series of the 5th, 10th, 25th, 50th, 75th, 90th, and 95th mean annual wind speed percentiles for each site were analyzed. Trends were evident in all percentiles but the largest magnitudes were characteristics of the weak and extreme percentiles.

5.2 Future work

Trend statistics for 9 coastal study sites are not sufficient to form robust conclusions about the spatial distribution of trends in mid-latitude coastal regions. Furthermore, a simple onshore versus offshore trend classification cannot mask underlying influences on wind speed such as the complex topography and physical processes. Additional work must be done in other coastal areas, not just regionally in Southeastern New England.

The calculation of wind speed trend magnitudes and signs is relatively straightforward, but diagnosing the trend source is more of an open-ended problem and not straightforward. Many factors, both intrinsic and extrinsic to the climate system influence wind speeds, and oftentimes those factors are difficult to quantify. Therefore, current research and published literature have not accurately attributed the sources of wind speed trend sources. Continued work must be devoted to determining the causes of such trends. I intend to continue to explore the possibility of a change in synoptic weather patterns through a power spectral density (PSD) analysis of regional wind speed data. I began an analysis of maximum monthly wind speeds to diagnose a possible change in storm frequency and intensity. Preliminary results indicate a significant change in 1 of the 3 parameters that characterize the Generalized Extreme Value distribution and a -0.0513$ms^{-1}a^{-1}$ trend in monthly maximum wind speed from the beginning to the end of the time series.

Determining the cause of wind speed trends can help scientists predict future wind speeds, which has importance in many fields. Wind energy assessment relies on an accurate understanding of wind speed and its spatial interannual variability. More importantly, the estimate of future wind speed regimes in climate models and projection of climate change scenarios is dependent on accurately quantifying and identifying causes of wind speed trends.

APPENDIX A

Acronyms

ABL Atmospheric Boundary Layer

AO Arctic Oscillation

ASOS Automated Surface Observing System

BIW Bimodal Weibull

CDO Climate Data Online

ENSO El Niño Southern Oscillation

GCM General Circulation Model

GEV Generalized Extreme Value

GOS Global Observing System

KAP Kappa

KG Knorr-Grilli

MCP Measure Correlate Predict

NCDC National Climatic Data Center

NAO North Atlantic Oscillation

NDBC National Data Buoy Center

NDVI Normalized Difference Vegetation Index

OLR Ordinary Linear Regression

OLR-AM Ordinary Linear Regression-Annual Means

OLR-DM Ordinary Linear Regression-Daily Means

PCA Principal Component Analysis

PDF Probability Density Function

PSD Power Spectral Density

RCM Regional Climate Model

SED Stream EDitor

WAK Wakeby

WASWind Wave-and Anemometer-Based Sea Surface Wind

WMO World Meteorological Organization

APPENDIX B

Weibull PDF Goodness of fit

The following figures are probability plots showing the goodness of fit of wind speed data and the Weibull PDF. The figures are on log-log scales, with the y-axes as probability and the x-axes as wind speed (m/s). The red dotted line indicates the Weibull PDF, and the blue plus signs are data. An ideal fit would include all data lying on the red PDF line. Figure B.1, Figure B.2, and Figure B.3 are the corresponding probability plots for the wind speed histograms and Weibull curves in Figures 11, Figure 12, and Figure 13 respectively.

Figure B.1 shows the Weibull fit of the hourly wind speed data at TF Green. Low and extreme high wind speed data fall below the probability curve, with the most drastic difference between the PDF and the wind speed data at low wind speed values. The artificial steps of 0.5m/s or whole knots are an artifact of the data coding. The Weibull goodness of fit for hourly mean data at B44011 is shown in Figure B.2. Generally there is a smooth fit and relatively low error except at the lowest wind speeds near the cut-in speed. Figure B.3 shows the Weibull probability plots for hourly mean wind speed data for each season at B44011. The fit for all seasons except winter is smooth and data falls along the red PDF line except for very weak wind speeds.

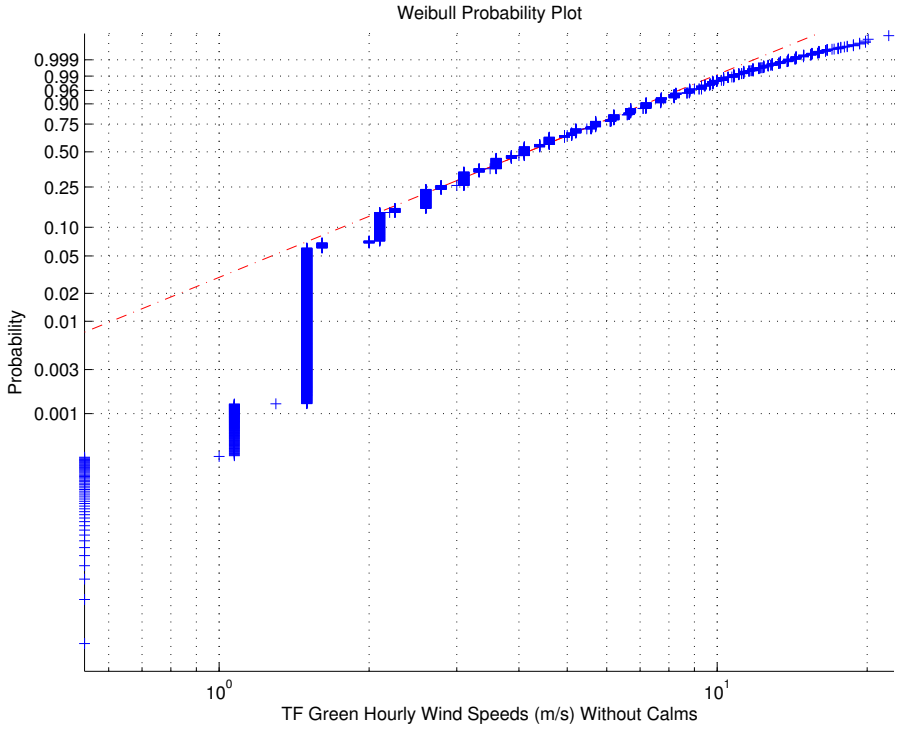

Figure B.1: Weibull probability plot for hourly wind speeds at TF Green. The red dashed line is the Weibull PDF data and the blue plus signs are the wind speed data (m/s) on log-log axes. Data with an ideal fit would lie on the red line with no deviations. The corresponding wind speed histogram and Weibull PDF are shown in Figure 11.

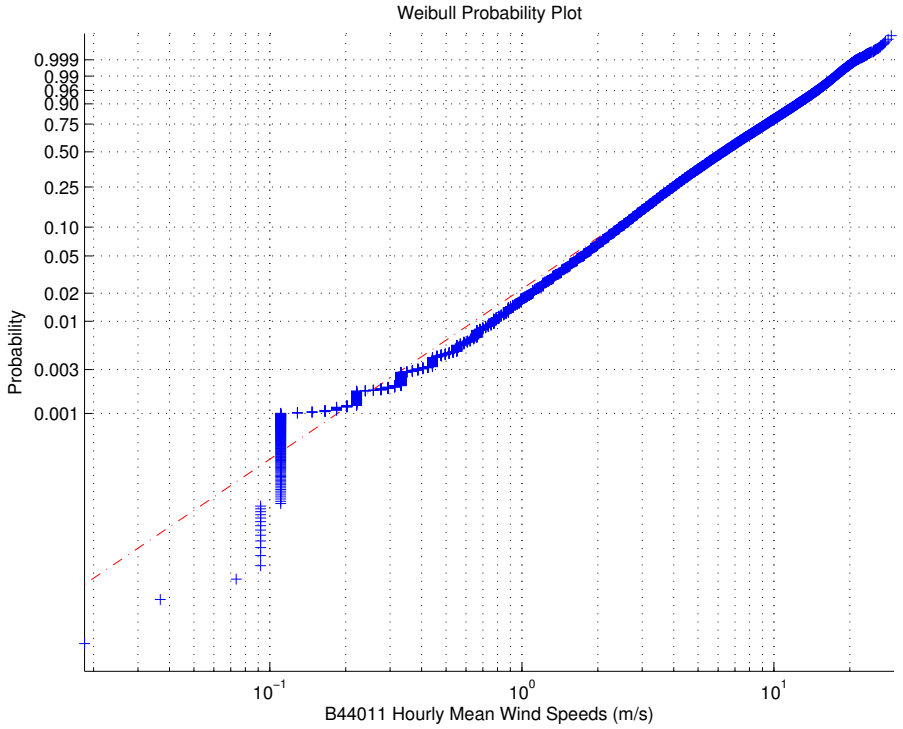

Figure B.2: Weibull probability plot for hourly mean wind speeds at B44011. The red dashed line is the Weibull PDF data and the blue plus signs are the wind speed data (m/s) on log-log axes. Data with an ideal fit would lie on the red line with no deviations. The corresponding wind speed histogram and Weibull PDF are shown in Figure 12.

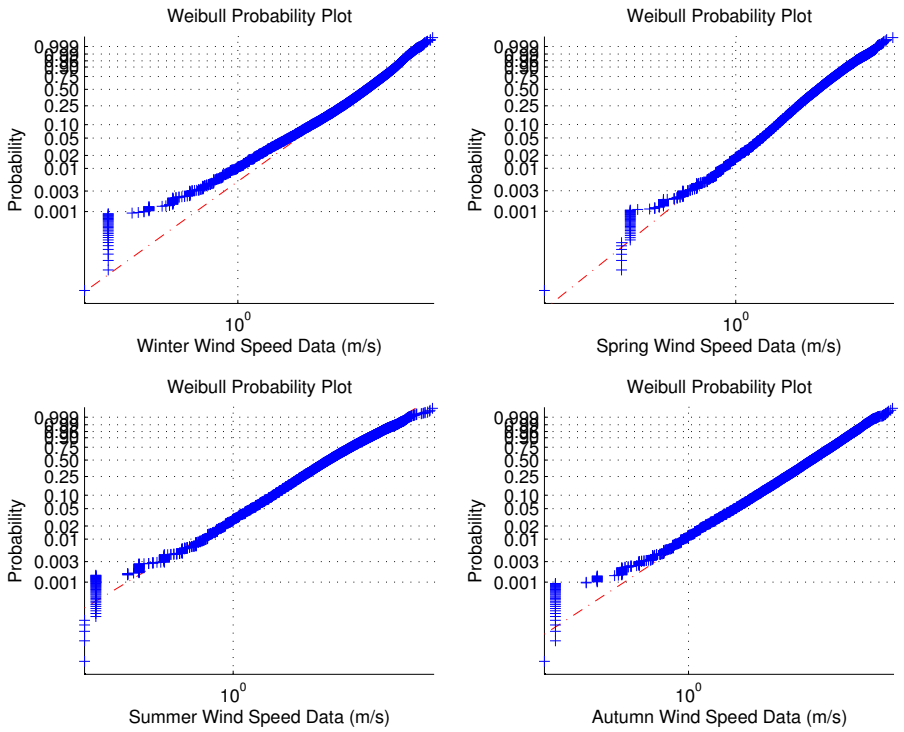

Figure B.3: Weibull probability plot for winter, spring, summer, and autumn hourly mean wind speeds at B44011. The red dashed line is the Weibull PDF data and the blue plus signs are the wind speed data (m/s) on log-log axes. Data with an ideal fit would lie on the red line with no deviations. Corresponding wind speed histograms and Weibull PDFs are shown in Figure 13.

BIBLIOGRAPHY

Aristidi, E., Agabi, K., Azouit, M., Fossat, E., Vernin, J., Travouillon, T., Lawrence, J. S., Meyer, C., Storey, J. W. V., Halter, B., Roth, W. L., and Walden, V. (2005). An analysis of temperatures and wind speeds above Dome C, Antarctica. *Astronomy and Astrophysics*, 430(2):739–746.

Baynes, C. and Davenport, A. (1975). Some statistical models for wind climate prediction. In *Preprints Fourth Conference Probability and Statistics in the Atmospheric Sciences*, pages 1–7, Tallahassee, FL. American Meteorological Society.

Bernard, S. M., Samet, J. M., Grambsch, A., Ebi, K. L., and Romieu, I. (2001). The potential impacts of climate variability and change on air pollution-related health effects in the United States. *Environmental Health Perspectives*, 109(2):1199–1209.

Bijl, W. (1997). Impact of a wind climate change on the surge in the southern North Sea. *Journal of Climate*, 8:45–59.

Brazdil, R., Chroma, K., Dobrovolny, P., and Tolasz, R. (2009). Climate fluctuations in the Czech Republic during the period 1961-2005. *International Journal of Climatology*, 29:223–242.

Brett, A. C. and Tuller, S. E. (1991). The autocorrelation of hourly wind speed observations. *Journal of Applied Meteorology*, 30:823–833.

Burn, D. H. and Hesch, N. M. (2007). Trends in evaporation for the Canadian prairies. *Journal of Hydrology*, 336(1-2):61–73.

Caires, S. and Sterl, A. (2005). 100-year return value estimates for ocean wind speed and significant wave height from the ERA-40 data. *Climate Research*, 18(7):1032–1048.

Cancino-Solorzano, Y. and Xiberta-Bernat, J. (2009). Statistical analysis of wind power in the region of Veracruz (Mexico). *Renewable Energy*, 34(6):1628–1634.

Capps, S. B. and Zender, C. S. (2008). Observed CAM3 GCM Sea Surface Wind Speed Distributions: Characterization, Comparison, and Bias Reduction. *Journal of Climate*, 21:6569–6585.

Cook, N. J. (1986). *Designer's Guide to Wind Loading of Building Structures Part 1: Background, Damage Survey, Wind Data & Structural Classification.* Butterworth-Heinemann.

Corti, S. (2012). Clustering Techniques and their applications at ECMWF. European Centre for Medium-Range Weather Forecasts.

Crosby, A. R. (2011). Offshore wind resource assessment with Standard Wind Analysis Tool (SWAT): A Rhode Island case study. Master's thesis, University of Rhode Island.

da Silva, V. P. R., e Silva, R. A., Cavalcanti, E. P., Braga, C. C., de Azevedo, P. V., Singh, V. P., and Pereira, E. R. R. (2010). Trends in solar radiation in NCEP/NCAR database and measurements in northeastern Brazil. *Solar Energy*, 84(10):1852–1862.

Diaconis, P. and Efron, B. (1983). Computer-intensive methods in statistics. *Scientific American*, 248:116–130.

Donelan, M., Drennan, W., Saltzman, E., and Wanninkhof, R., editors (2002). *Gas Transfer at Water Surfaces*, volume 127 of *Geophysical Monograph Series*. American Geophysical Union.

Donohue, R. J., McVicar, T. R., and Roderick, M. L. (2009). Climate-related trends in Australian vegetation cover as inferred from satellite observations, 1981-2006. *Global Change Biology*, 15(4):1025–1039.

Emery, W. J. and Thompson, R. E. (2001). *Data Analysis Methods in Physical Oceanography*. Elsevier, 2 edition.

Fuentes, M. C. (2005). Los temporales de lluvia y viento en Galicia; Propuesta de clasificacion y analisis de tendencias (1961-2001). *Investigation Geography*, 36:103–118. in Spanish.

Fujii, T. (2007). On geographical distributions and decadal changes of the annual maximum wind speeds caused by typhoons in Japan. *Journal of Natural Disaster Science*, 26(3):267–277.

George, S. S. and Wolfe, S. A. (2009). El niño stills winter winds across the southern canadian prairies. *Geophysical Research Letters*, 36(23):L23806.

Glover, D. M., Jenkins, W. J., and Doney, S. C. (2011). *Modeling Methods for Marine Science*. Cambridge.

Greene, J. S., Chatelain, M., Morrissey, M., and Stadler, S. (2012a). Estimated changes in wind speed and wind power density over the western High Plains 1971-2000. *Theoretical and Applied Climatology*, 109:507–518.

Greene, J. S., Chatelain, M., Morrissey, M., and Stadler, S. (2012b). Projected Future Wind Speed and Wind Power Density Trends over the Western US High Plains. *Atmospheric and Climate Sciences*, 2:32–40.

Grilli, A. and Spaulding, M. (2010). Evaluation of wind energy resources in southern RI coastal waters for wind energy development. Ocean SAMP.

Grilli, A. and Spaulding, M. (2013). Spatial variability of the offshore wind resource in Rhode Island. submitted.

Groisman, P. Y. (2002). Data documentation for data set DSI-6421: Enhanced hourly wind station data for the contiguous United States. National Climatic Data Center, Asheville, N. C.

Guo, H., Xu, M., and Hu, Q. (2011). Changes in near-surface wind speed in China: 1969-2005. *International Journal of Climatology*, 31(3):349–358.

He, Y., Monahan, A. H., Jones, C. G., Dai, A., Biner, S., Caya, D., and Winger, K. (2010). Probability distributions of land surface wind speeds over north america. *Journal of Geophysical Research*, 115(D4):D04103.

Hennessey, J. P. (1977). Some Aspects of Wind Power Statistics. *Journal of Applied Meteorology*, 16(2):119–128.

Hewston, R. and Dorling, S. R. (2011). An analysis of observed daily maximum wind gusts in the UK. *Journal of Wind Engineering and Industrial Aerodynamics*, 99(8):845–856.

Iacono, M. J. (2009). Why is the Wind Speed Decreasing? Blue Hill Meteorological Observatory.

Jungo, P., Goytette, S., and Beniston, M. (2002). Daily wind gust speed probabilities over Switzerland according to three types of synoptic circulation. *International Journal of Climatology*, 22:485–499.

Justus, C., Hargraves, W., and Yalcin, A. (1976). Nationwide assessment of potential output from wind powered generators. *Journal of Applied Meteorology*, 15:673–678.

Klink, K. (1999). Trends in mean monthly maximum and minimum surface wind speeds in the coterminous United States, 1961-1990. *Climate Research*, 13:193–205.

Klink, K. (2002). Trends and Interannual Variability of Wind Speed Distributions in Minnesota. *Journal of Climate*, 15:3311–3317.

Klink, K. (2007). Atmospheric Circulation Effects on Wind Speed Variability at Turbine Height. *Journal of Applied Meteorology and Climatology*, 46:445–456.

Kondrashov, D. and Ghil, M. (2006). Spatio-temporal filling of missing points in geophysical data sets. *Nonlinear Processes in Geophysics*, 13:151–159.

Kruger, A. C., Goliger, A. M., Retief, J. V., and Sekele, S. (2010). Strong wind climatic zones in South Africa. *Wind and Structures*, 13(1):37–55.

Liu, J. G., Li, S. X., Ouyang, Z. Y., Tam, C., and Chen, X. D. (2008). Ecological and socioeconomic effects of China's policies for ecosystem services, 1981-2006. *Proceedings of the National Academy of Sciences of the USA*, 105(28):9477–9482.

Lu, L., Yang, H., and Burnett, J. (2002). Investigation on wind power potential on hong kong islands-an analysis of wind power and wind turbine characteristics. *Renewable Energy*, 27(1):1–12.

Lynch, A. H., Curry, J. A., Brunner, R. D., and Maslanik, J. A. (2004). Toward an integrated assessment of the impacts of extreme wind events on Barrow, Alaska. *Bulletin of the American Meteorological Society*, 85(2):209–221.

Mahowald, N. M., Ballantine, J. A., Feddema, J., and Ramankutty, N. (2007). Global trends in visibility: implications for dust sources. *Atmospheric Chemistry and Physics*, 7(12):1852–1862.

Mahowald, N. M., Engelstaedter, S., Luo, C., Sealy, A., Artaxo, P., Benitez-Nelson, C., Bonnet, S., Chen, Y., Chuang, P. Y., Cohen, D. D., Dulac, F., Herut, B., Johansen, A. M., Kubilay, N., Losno, R., Maenhaut, W., Paytan, A., Prospero, J. M., Shank, L. M., and Siefert, R. L. (2000). Atmospheric Iron Deposition: Global Distribution, Variability, and Human Perturbations. *Annual Review of Marine Science*, 1:245–278.

Matsoukas, C., Benas, N., Hatzianastassiou, N., Pavlakis, K. G., Kanakidou, M., and Vardavas, I. (2011). Potential evaporation trends over land between 1983-2008: driven by radiative fluxes or vapour-pressure deficit? *Atmospheric Chemistry and Physics*, 11(15):7601–7616.

McKee, T. B., Doesken, N. J., Davey, C. A., and Pielke, R. A. (2000). Climate Data Continuity with ASOS. Colorado Climate Center, Colorado State University.

McVicar, T. R., Roderick, M. L., Donohue, R. J., Li, L. T., Niel, T. G. V., Thomas, A., Grieser, J., Jhajharia, D., Himri, Y., Mahowald, N. M., Mescherskaya, A. V., Kruger, A. C., Rehman, S., and Dinpashoh, Y. (2012). Global review and synthesis of trends in observed terrestrial near-surface wind speeds: Implications for evaporation. *Journal of Hydrology*, 416-417:182–205.

McVicar, T. R., Van Niel, T. G., Li, L. T., Roderick, M. L., Rayner, D. P., Ricciardulli, L., and Donohue, R. J. (2008). Wind speed climatology and trends for australia, 1975–2006: Capturing the stilling phenomenon and comparison with near-surface reanalysis output. *Geophysical Research Letters*, 35(20):L20403.

Merrill, J. T. and Knorr, K. I. (2012). Wind Resource Assessment Technical Report. University of Rhode Island Graduate School of Oceanography.

Mescherskaya, A. V., Ermin, V. V., Baranova, A. A., and Maystrova, V. V. (2006). Change in wind speed in northern Russia in the second half of the twentieth century, from surface and upper air data. *Russian Meteorology and Hydrology*, 9:46–58.

Mikhail, A. S. (1985). Height extrapolation of wind data. *Journal of Solar Energy Engineering*, 107:10–14.

Monahan, A. H. (2006). The probability distribution of sea surface wind speeds. Part I: Theory and sea winds observations. *Journal of Climate*, 19:497–520.

Morgan, E. C., Lackner, M., Vogel, R. M., and Baise, L. G. (2011). Probability distributions for offshore wind speeds. *Energy Conversion and Management*, 52:15–26.

Nadolski, V. L. (1998). Automated Surface Observing System (ASOS) User's Guide. National Oceanic and Atmospheric Administration.

Oke, T. R. (2002). *Boundary Layer Climates*. Routledge, 2 edition.

Okubo, A. and Levin, S. A. (1989). A theoretical framework for data-analysis of wind dispersal of seeds and pollen. *Ecology*, 70(2):329–338.

O'Neal, M., Nearing, M., Vining, R., Southworth, J., and Pfeifer, R. (2005). Climate change impacts on soil erosion in Midwest United States with changes in crop management. *Catena*, 61:165–184.

Peterson, E. W. and Hennessey, J. P. (1978). On the use of power laws for estimates of wind power potential. *Journal of Applied Meteorology*, 17:390–394.

Pilson, M. E. Q. (2008). Narragansett bay amidst a globally changing climate. In Desbonnet, A. and Costa-Pierce, B. A., editors, *Science for Ecosystem-Based Management*, chapter 2, pages 35–46. Springer.

Pryor, S. and Barthelmie, R. (2009). Historical trends in near-surface wind speeds. In *Understanding Climate Change*, chapter 15, pages 169–183. Indiana University Press.

Pryor, S. and Ledolter, J. (2010). Addendum to wind speed trends over the contiguous united states. *Journal of Geophysical Research*, 115(D10):D10103.

Pryor, S. C., Barthelmie, R. J., Young, D. T., Takle, E. S., Arritt, R. W., Flory, D., Gutowski, W. J., Nunes, A., and Roads, J. (2009). Wind speed trends over the contiguous United States. *Journal of Geophysical Research*, 114:D14105.

Rayner, D. P. (2007). Wind run changes: The dominant factor affecting pan evaporation trends in Australia. *Journal of Climate*, 20(14):3379–3394.

Recio, M., Rodriguez-Rajo, R. J., Jato, M. V., Trigo, M. M., and Cabequdo, B. (2009). The effect of recent climatic trends on Urticaceae pollination in two bioclimatically different areas in the Iberian Peninsula: Malaga and Vigo. *Climatic Change*, 97(1-2):215–228.

Ren, D. (2010). Effects of global warming on wind energy availability. *Journal of Renewable and Sustainable Energy*, 2:052301.

Roderick, M. L., Rotstayn, L. D., Farquhar, G. D., and Hobbins, M. T. (2007). On the attribution of changing pan evaporation. *Geophysical Research Letters*, 34(17):L17403.

Rogers, A. L., Rogers, J. W., and Manwell, R. F. (2005). Uncertainties in Results of Measure-Correlate-Predict Analyses. In *American Wind Energy Association Conference*.

Sedefian, L. (1980). On the vertical extrapolation of mean wind power density. *Journal of Applied Meteorology*, 19(4):488–493.

Seidel, D. J., Fu, Q., Randel, W. J., and Reichler, T. J. (2008). Widening of the tropical belt in a changing climate. *Nature Geoscience*, 1:21–24.

Smits, A., Klein-Tank, A. M. G., and Konnen, G. P. (2005). Trends in storminess over the Netherlands, 1962-2002. *International Journal of Climatology*, 25:1331–1344.

Spiegel, M. and Stephens, L. (2011). *Statistics*. Schaum's outlines. McGraw Hill, 4 edition.

Sweeney, J. (2000). A three-century storm climatology for Dublin 1715-2000. *Investigation Geography*, 33(1):1–14.

Thomas, B. R., Kent, E. C., Swail, V. R., and Berry, D. I. (2008). Trends in ship wind speeds adjusted for observation method and height. *International Journal of Climatology*, 28(6):747–763.

Thomas, B. R. and Swail, V. R. (2011). Buoy wind inhomogeneities related to averaging method and anemometer type: application to long time series. *International Journal of Climatology*, 31(7):1040–1055.

Tokinaga, H. and Xie, S. P. (2011). Wave and anemometer-based sea-surface wind (WASWind) for climate change analysis. *Journal of Climate*, 24(1):267–285.

Touma, J. S. (1977). Dependence of the wind profile power law on stability for various locations. *Journal of Air Pollution Control Association*, 27:863–866.

Turner, J., Colwell, S., Marshall, G., Lachlan-Cope, T., Carleton, A., Jones, P., Lagun, V., Reid, P., and Iagovkina, S. (2005). Antarctic climate change during the last 50 years. *International Journal of Climatology*, 25(3):279–294.

Vautard, R., Cattiaux, J., Yiou, P., Thepaut, J., and Ciais, P. (2010). Northern Hemisphere atmospheric stilling partly attributed to an increase in surface roughness. *Nature Geoscience*, 3:756–761.

Wan, H., Wang, X. L., and Swail, V. R. (2009). Homogenization and Trend Analysis of Canadian Near-Surface Wind Speeds. *Journal of Climate*, 23:1209–1225.

Wanninkhof, R., Doney, S. C., Takahashi, T., and McGillis, W. R. (2002). The effect of using time-averaged winds on regional air-sea CO_2 fluxes. In *Gas Transfer at Water Surfaces*, volume 127 of *Geophysical Monograph Series*, pages 351–356. American Geophysical Union.

Wever, N. (2012). Quantifying trends in surface roughness and the effect on surface wind speed observations. *Journal of Geophysical Research*, 117(D11):D11104.

Wieringa, J., Davenport, A., Grimmond, C. S. B., and Oke, T. R. (2001). New revision of davenport roughness classification. In *paper presented at Third European and African Conference on Wind Engineering*, pages 1–7, University of Eindhoven, Eindhoven, Netherlands.

Wilks, D. S. (2011). *Statistical Methods in the Atmospheric Sciences*. Elsevier, 3 edition.

Xu, M., Chang, C.-P., Fu, C., Qi, Y., Robock, A., Robinson, D., and Zhang, H.-m. (2006). Steady decline of east asian monsoon winds, 1969–2000: Evidence from direct ground measurements of wind speed. *Journal of Geophysical Research*, 111:D24111.

Yan, Z., Bate, S., Chandler, R. E., Isham, V., and Wheater, H. (2002). An analysis of daily maximum wind speed in northwestern Europe using generalized linear models. *Journal of Climate*, 15(15):2073–2088.

Yin, J. H. (2005). A consistent poleward shift of the storm tracks in simulations of 21st century climate. *Geophysical Research Letters*, 32(18):L18.

Young, I. R., Zieger, S., and Babanin, A. V. (2011). Global Trends in Wind Speed and Wave Height. *Science*, 332:451–455.